Optimal control of aging in complex networks

Eric D. Sun[a,1], Thomas C. T. Michaels[a,1], and L. Mahadevan[a,b,c,2]

[a]School of Engineering and Applied Sciences, Harvard University, Cambridge, MA 02138; [b]Department of Physics, Harvard University, Cambridge, MA 02138; and [c]Department of Organismic and Evolutionary Biology, Harvard University, Cambridge, MA 02138

Edited by John A. Rogers, Northwestern University, Evanston, IL, and approved July 7, 2020 (received for review April 5, 2020)

Many complex systems experience damage accumulation, which leads to aging, manifest as an increasing probability of system collapse with time. This naturally raises the question of how to maximize health and longevity in an aging system at minimal cost of maintenance and intervention. Here, we pose this question in the context of a simple interdependent network model of aging in complex systems and show that it exhibits cascading failures. We then use both optimal control theory and reinforcement learning alongside a combination of analysis and simulation to determine optimal maintenance protocols. These protocols may motivate the rational design of strategies for promoting longevity in aging complex systems with potential applications in therapeutic schedules and engineered system maintenance.

aging | control | networks | failure | repair

Aging is the process of damage accumulation with time that is responsible for an increasing susceptibility to death or decay (1). Many complex systems that consist of multiple interacting components (2) (e.g., biological organisms and artificially engineered systems) experience aging. Indeed, models of the interdependence between components of a system implemented in a network (3) show aspects of aging and eventual system-wide catastrophe and death. This is because when components are interdependent, the failure of one component may adversely affect its dependents. The dynamics of these processes have been the focus of many recent studies (4–7), exhibit temporal scaling (8, 9) and failure cascades, and reproduce empirical survivorship curves for many biological organisms and technological devices (4).

Understanding the onset of aging in network models points toward a central question in the field (10): how can one control aging in complex systems through interventions associated with repair and maintenance, with the eventual goal of designing strategies for increasing longevity? Available control strategies in networks are primarily for single nodes (11) and sets of driver nodes (12, 13), and they largely fall into three classes: network design (14, 15), edge and node removal at onset of cascade (16), and time-dependent edge weight distribution (17, 18). Complementing these approaches, in reliability engineering, there are maintenance policies for deteriorating multiunit systems (19–22) that include opportunistic repair (23) and group and block replacement (24) for systems with economic and structural dependencies between components (20, 21, 25). However, aging systems are primarily characterized by failure dependencies between components. Only very special repair policies have been optimized for failure-dependent complex systems (26), and most are restricted to systems composed of few units (20, 21), or with strong assumptions about the underlying failure distribution without consideration for the dynamics of individual network components from which they emerge (22, 27).

Here, we deploy an optimal control framework to determine strategies to delay aging in a tractable and realistic model for the failure of interdependent networks (4). A combination of numerical simulations and analysis shows how the microscopic dynamics of individual network components that are capable of stochastic failure determine how system-level macroscopic dynamics of decreasing vitality and failure cascades follow. We then introduce the notion of repair in such a network that can lead to a delay in aging, but at a cost. This can be couched in the framework of optimal control theory (28) and allows us to determine strategies to delay aging in these interdependent networks analytically in the linearized regime and computationally in the nonlinear regime. To understand the implications of our results, we then deploy a simple reinforcement learning scheme (29) to determine the parameters associated with explicit temporal repair protocols that determine the efficacy of drugs on the longevity of a classic model organism used in aging studies—the nematode *Caenorhabditis elegans*.

Network Model of Aging and Repair

Computational Model. Our computational model of aging starts with the consideration of a network with N nodes representing the individual components of the complex system and edges between nodes representing interdependencies between the individual components (Fig. 1*A*). The main network structure used in this study is the Gilbert $G(N,p)$ random graph (30); in this network, edges between any two nodes occur with probability p, where the mean node degree is $z=p(N-1)$. We also explore Erdős–Rényi $G(N,m)$ random networks (31) and Barabási–Albert scale-free networks (32); these structures produce qualitatively similar results as compared with the Gilbert random graph (*SI Appendix*, Fig. S6). In the model, each node is assigned an initial state of binary value $x_i \in \{0,1\}$ with probabilities $P(x_i=0)=d$ and $P(x_i=1)=1-d$, where d denotes the prenatal damage of the complex system at birth. The state of a node represents its functionality, where $x_i=1$ denotes a vital, functional ith node and $x_i=0$ denotes a dead, failed ith node.

The network is then allowed to age via a simple iterative algorithm (*SI Appendix*, Algorithm 1) through the following actions: 1) each node fails with probability f; 2) nodes are repaired with probability r; 3) a node fails if the fraction of vital providers (i.e., functional neighboring nodes) is less than I; 4) the network

Significance

Aging in many complex systems composed of interacting components leads to decay and eventual collapse/death. Repair delays this process at a cost, suggesting a trade-off between the cost of repair and the benefit of health and longevity. Using an interdependent network model of a complex system, we introduce a control theoretic and learning framework for maximizing longevity at minimal repair cost and determine the optimal maintenance schedule for the system. Our approach should be relevant to determining checking schedules for complex engineered and living systems.

Author contributions: E.D.S., T.C.T.M., and L.M. designed research, performed research, contributed new reagents/analytic tools, analyzed data, and wrote the paper.

The authors declare no competing interest.

This article is a PNAS Direct Submission.

[1]E.D.S. and T.C.T.M. contributed equally to this work.

[2]To whom correspondence may be addressed. Email: lmahadev@g.harvard.edu.

This article contains supporting information online at https://www.pnas.org/lookup/suppl/doi:10.1073/pnas.2006375117/-/DCSupplemental.

First published August 12, 2020.

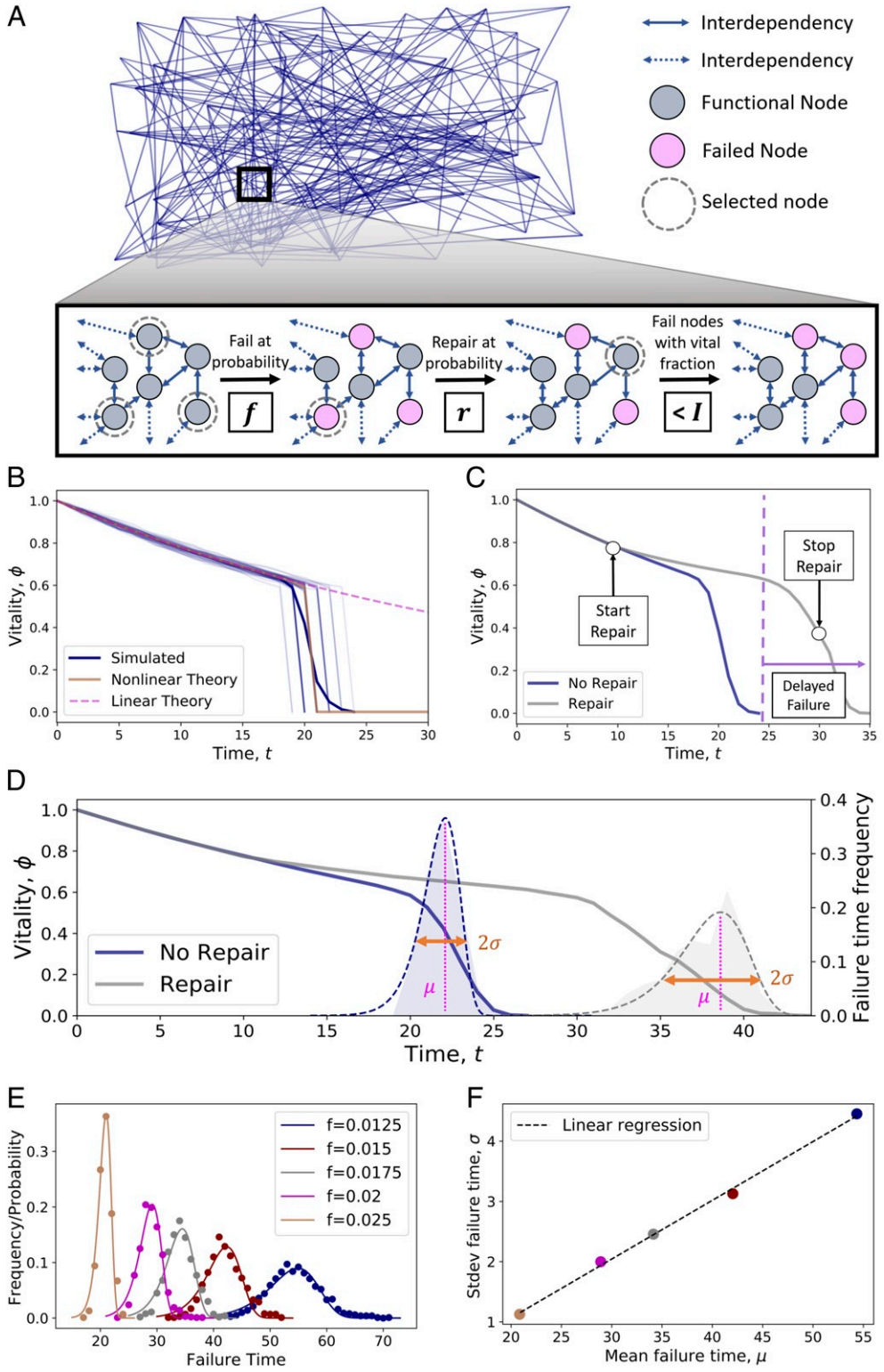

Fig. 1. Computational network model of aging and repair. (*A*) Schematic representation of the network model of aging, represented by a network, where nodes denote components and edges denote interdependencies between these components. The network aging algorithm is portrayed in a smaller subsection of the network. At each time step, nodes are failed with probability f, repaired with probability r, and failed if their fraction of vital providers is less than I. (*B*) Simulated cascading failures in a Gilbert random model ($p = 0.1$, $N = 1{,}000$, $f = 0.025$, $r = 0$, $d = 0$, $I = 0.5$). Faint blue lines refer to 50 individual vitality trajectories; the solid blue line is the mean vitality $\Phi(t)$; the dashed magenta line is the analytic solution to the linear model, Eq. **5**, where $I = 0$; and the solid gold line is the numeric solution to the nonlinear model, Eq. **4**. (*C*) Network repair at $r = 0.025$ from $T_1 = 10$ to $T_2 = 40$ (gray) delays network failure and improves mean vitality for 1,000 networks as compared with nonrepaired networks (blue). (*D–F*) Fluctuation of failure times. (*D*) Optimal repair results in increased network failure time variance (gray) as compared with no repair (dark blue). Parameters: $f = 0.025$, $r = 0.01$, $\alpha = 10$. Also shown are the mean failure time μ and the standard deviation σ in the absence and presence of repair. (*E*) Network failure time distributions for different values of f are described by the Weibull distribution (solid lines) (see *SI Appendix*, section S3). (*F*) Linear regression (dotted line; slope = 0.0975) of mean μ and SD σ of network failure times for different values of f.

vitality is calculated using the expression $\phi(t) = \frac{1}{N}\sum_{i=1}^{N} x_i$; and 5) the system fails if $\phi(t) < 0.1$ (Fig. 1*A*). Here, I is a measure of the interdependence between the system components and denotes the threshold fraction of vital providers required for a node to stay alive. $I = 0$ corresponds to a collection of N independent components, and if the vital fraction is less than I, then the node automatically fails.

Our model reproduces the characteristic cascading failures that are present in the computational models of breakdown of complex systems (4, 14, 16, 33). In a representative simulation, the vitality $\phi(t)$ of the system decreases slowly in the linear regime before collapsing rapidly after a critical vitality value, ϕ_c (Fig. 1*B*). The cascading failure is observed in all three graph structures (*SI Appendix*, Fig. S6). This sudden decrease in system vitality is similar to the compression of morbidity that is observed during late life for humans and many other biological organisms (34). Movie S1 shows a two-dimensional visualization of network failure. Our simulations allow us to go beyond the mean-field theory and look at the probability distribution of failure events, defined in Fig. 1*D* in terms of the mean time for failure μ and the standard deviation in the failure time σ. In Fig. 1*E*, we show how these parameters vary with the failure rate f, and in Fig. 1*F*, we see that the standard deviation is linearly correlated with the mean failure time, consistent with a Weibull distribution (see *SI Appendix*, section S3).

Nonlinear Theory of Network Aging. To complement our computational model of aging networks, we also construct an effective equation for the average network vitality measured over several realizations, $\Phi(t) = \langle \phi(t) \rangle$. A mean-field model for the average vitality as a function of time may then be written as

$$\frac{d\Phi}{dt} = -f_{\text{tot}}\Phi + r_{\text{tot}}(1-\Phi), \qquad [1]$$

where $f_{\text{tot}}\Phi$ is the total rate of node failure and $r_{\text{tot}}(1-\Phi)$ is the total rate of repair. It is important to note that f_{tot} and r_{tot} denote the collective aspects of the network and are thus different from the respective intrinsic failure and repair rates f and r of nodes. They thus account for interdependence between nodes. To understand the relation between these variables, we note that a node fails for one of two reasons: 1) it fails with intrinsic rate f, or 2) it fails if the fraction of its vital providers falls below I (i.e., failure cascade). At leading order in failure rate f, we can neglect the simultaneous failure of two or more nodes at any time point; hence, induced failure occurs in one step, when the node is left with the minimum number of vital providers, and then, one of these vital providers fails. The total rate of node failure is thus given by the sum of the intrinsic failure rate $f\Phi$ and the rate of failure of the last vital provider $f_{\text{tot}}\Phi = f\Phi + k(1-f)\, f_{\text{tot}}\, m(I,\Phi)\Phi$, where $k = zI$ is the minimum number vital providers required for a node to function, $z = p(N-1)$ is the average number of edges between nodes (for a Gilbert random graph), and

$$m(I,\Phi) = \binom{z}{k}\Phi^k(1-\Phi)^{z-k} \qquad [2]$$

describes the (mean-field) probability that a node is left with k vital providers. We thus obtain the total rate of failure as $f_{\text{tot}} = \frac{f}{1-km(I,\Phi)(1-f)}$. Similar arguments can be employed to determine the total rate of repair. A node can be repaired only if the following two conditions are met: 1) the node is failed, and 2) the node is connected to at least the minimum fraction I of vital providers required for it to function after repaired. The total rate of repair is thus the product of the intrinsic rate of repair, $r(1-\Phi)$, and the probability $h(I,\Phi)$ that the node is connected to at least $k = zI$ vital providers:

$$h(I,\Phi) = \sum_{j=k}^{z}\binom{z}{j}\Phi^j(1-\Phi)^{z-j}. \qquad [3]$$

In summary, we arrive at

$$\frac{d\Phi}{dt} = -\frac{f\Phi}{1-km(I,\Phi)(1-f)} + r\,h(I,\Phi)(1-\Phi), \qquad [4]$$

where f and r are the intrinsic frequencies of failure and repair, respectively, and interdependence between nodes is captured in this mean-field equation by the nonlinear functions $m(I,\Phi)$ and $h(I,\Phi)$. In *SI Appendix*, Fig. S1, we compare the mean-field model Eq. **4** and the network simulations (Fig. 1*B*). Analytically, we see that the solution to Eq. **4** describes an average vitality that decreases slowly at early times. In the limit when the system is away from collapse ($ft \ll 1$), Eq. **4** can be linearized and approximated to leading order as

$$\frac{d\Phi}{dt} = -f\Phi + r(1-\Phi). \qquad [5]$$

This leads to an exponentially decaying vitality (Fig. 1*B*). At later times, the average vitality exhibits failure cascade and rapid collapse after a critical vitality value Φ_c is reached (Fig. 1*B*). This effect originates when the denominator in the first term on the right-hand side of Eq. **4** becomes small, which causes the effective failure rate to blow up; thus, an estimate for the critical fraction for failure cascade can be obtained by maximizing $m(I,\Phi)$ over Φ, which yields $\Phi_c = I$ (*SI Appendix*, section S1).

Optimal Control of Network Aging

Having a qualitative understanding of the forward problem of how aging arises in interdependent networks, we now turn to the problem of controlling the progressive aging of a network by varying the repair rate, subject to some constraints.

Optimal Repair Protocols. For an interdependent network that ages according to Eq. **4**, our goal is to design optimal repair protocols [i.e., replace the constant repair frequency r in Eq. **4** by a time-dependent unknown repair rate $r(t)$ to regulate network vitality]. Since high vitality is expected to correspond to a "benefit," while repair actions come with a "cost," we introduce the following cost function to capture this balance between network vitality and repair:

$$\text{Cost} = \int_0^T e^{-\gamma t}\,\mathcal{C}(\Phi(t), r(t))\,dt, \qquad [6]$$

where T is the final time and $\mathcal{C}$ is a monotonically decreasing function of vitality $\Phi(t)$ and a monotonically increasing function of repair $r(t)$. The exponential term describes the situation when future values of the cost are discounted, where $\gamma \geq 0$ is the discount rate. To balance the cost of repair and the benefit of vitality, we focus here on a simple linear cost function $\mathcal{C} = \alpha\, r(t) - \Phi(t)$, where α is the relative cost of repair. The first term describes the total cost for repair as the integral of the repair protocol in time, while the second term is the gain from vitality; the constant α describes the relative importance of the two terms in the cost function. The goal of the optimal control problem defined by Eqs. **4** and **6** is to find the repair protocol $r(t)$ that minimizes the cost function Eq. **6** while satisfying the evolution equation for vitality Eq. **4** (*SI Appendix*, section S8 has a discussion of alternative cost functions and the effect of nonlinear cost functionals).

We solve this optimal control problem for a network with initial vitality $\Phi(t=0) = 1-d$ using the framework of optimal control theory and Pontryagin's principle (28) (*SI Appendix*, section S2 has details). Since the optimal control problem is linear in

the repair rate $r(t)$, the optimal repair protocol will correspond to a bang-bang control that switches between $r(t)=0$ (no repair) and $r(t)=r$ (maximal repair). Repair is turned on when

$$h(I,\Phi)(1-\Phi) > \frac{\alpha}{|\lambda|}, \qquad [7]$$

where λ is a time-dependent costate variable, which is determined as the solution to *SI Appendix*, Eq. **S23** (*SI Appendix*, section S2.2 has a derivation, and *SI Appendix*, section S2.4 has a discussion on singular arcs). Eq. **7** states that the optimal decision to repair depends on two parameters: 1) the repairable fraction of nodes, $h(I,\Phi)(1-\Phi)$, and 2) a time-dependent threshold $\alpha/|\lambda|$, which depends on the relative cost of repair α. The repairable fraction increases with time as nodes in the network fail and/or become increasingly susceptible to failure cascades; on the other hand, the threshold for the repairable fraction also increases with time as the system ages, leading to a smaller window of repair.

Linear Control Theory. To gain an understanding of how the optimal repair protocol depends on the physical parameters, we focus first on the linearized limit, Eq. **5**, valid away from vitality collapse. In fact, explicit analytical expressions for optimal protocols can be obtained in this case. Condition Eq. **7** leads to nonmonotonic optimal repair protocols characterized by a waiting time for repair, followed by an intermediate period where repair is preferable and a terminal phase where the repair rate is set again to zero (*SI Appendix*, Fig. S2):

$$r(t) = \begin{cases} 0, & t < T_1 \text{ and } t > T_2 \\ r, & T_1 < t < T_2 \end{cases}, \qquad [8]$$

where T_1 and T_2 are switching times, given by (*SI Appendix*, section S2 has a derivation)

$$T_1 \simeq \frac{1}{f}\log\left[\frac{1-d}{1-\alpha(f+r+\gamma)}\right] \qquad [9a]$$

$$T_2 \simeq T - \frac{1}{f+\gamma}\log\left[\frac{1}{1-\alpha(f+r)(f+\gamma)/f}\right]. \qquad [9b]$$

The dependence of T_1 and T_2 on the failure rate f, repair rate r, and cost of repair α is shown in Fig. 2. The optimal repair protocol in time consists of an initial phase when system vitality is high and no repair is necessary and a repair period that is initiated at time T_1 and persists until time T_2. For $\gamma=0$ and $d=0$ (corresponding to a healthy organism), the repair protocol is symmetric with respect to the end time T since $T_1 = T - T_2$. The protocol is no longer symmetric with respect to T when $d>0$; in particular, while the initial vitality level does not affect the end time T_2, the start time T_1 decreases with increasing d, implying that the optimal repair protocol starts earlier and lasts for longer as the initial vitality of the system decreases. There is a critical value for initial vitality, $\Phi(t=0) < 1-d_c = 1-\alpha(f+r+\gamma)$, below which the optimal repair protocol starts right away. Robust achievability of optimal protocols depends on the curvature of the cost function around the optimum Eq. **9**, which for $\gamma=0$ is given by $\simeq fr[1-\alpha(f+r)]/(f+r)$ (*SI Appendix*, section S2.3.1). We also characterized longevity gain resulting from optimal protocols as a function of α and γ (*SI Appendix*, Fig. S3).

In the infinite horizon limit $T\to\infty$ and $\gamma>0$, we enter a regime where the optimal solution for repair maximizes the discounted health of the system over an indefinite period under a cost constraint. Biologically, this is equivalent to optimizing longevity as compared with health span for finite T, while considering a discount factor resulting from extrinsic mortality (35). Since $T_2\to\infty$, the infinite horizon repair protocol is characterized by a single switching time T_1, after which the system is repaired in perpetuity.

Thus far, we have focused on the simple linear cost function. Exploring nonlinear cost functions leads to optimal repair protocols that are no longer of bang-bang type but are still nonmonotonic in time (*SI Appendix*, section S8), with initial and terminal phases of low repair and an intermediate region of higher repair (*SI Appendix*, Fig. S8). Additional extensions may be motivated by future experiments and might involve considering a terminal cost for vitality, including nonlinearities in vitality and/or repair rate (*SI Appendix*, section S8), or introducing additional variables, such as node checking and associated cost (*SI Appendix*, section S9).

Phase Diagram for Repair. A question of some interest is the determination of the conditions under which a repair protocol is advisable. From Eq. **9**, it follows that since T_1 must, by definition, be smaller than T_2, a repair protocol exists for $d=0$ and $\gamma=0$ only if

$$fT \geq 2\log\left[\frac{1}{1-\alpha(f+r)}\right]. \qquad [10]$$

Eq. **10** results in a phase diagram separating a region of "repair" from a region of "no repair," where repair is too costly, as a function of two relevant dimensionless parameters $\alpha(f+r)$ and fT. As a function of failure frequency f and at constant values of α, r, and T, Eq. **10** predicts the existence of regions of low ($fT\ll 1$) and high failure rates ($fT\gg 1$), respectively, where the best option is no repair (Fig. 2*B*). This behavior follows intuition; when failure rate is low, vitality remains high over the interval $[0, T]$, such that the cost of repair would be unnecessarily large compared with the benefit associated with increased vitality. Similarly, when the failure rate is large, a significant improvement of vitality would require an insurmountable cost of repair. As the repair rate r increases, Eq. **10** predicts a rapidly shrinking window of repair due to the combined effect of increasing the effectiveness of and associated cost (αr) of repair (Fig. 2*C*). As the cost of repair α increases, Eq. **10** similarly predicts a decreasing window of repair (Fig. 2*D*) that results from an increasing cost burden. There exists a critical value for the repair cost, $\alpha_c = 1/(f+r)$, above which there is no repair.

Interdependent Networks. For networks with interdependent components, the optimal protocols are still bang bang, and the switching times can be calculated using Eq. **7**. Notably, increasing the interdependence ($I\geq 0$) between components provided qualitatively similar strategies for maintaining optimal health span (finite T) as the linear theory. Our theory predicts that the window of repair increases with interdependence in order to compensate for the accelerated aging and reduced response to repair in interdependent networks. Increasing I has little effect on the switching time T_1 since at high vitality, the interdependent system is close to the linear theory. However, as I increases, the repairable fraction $h(\Phi, I)$ and the effective repair rate decrease monotonically with I for fixed Φ, which results in an increasing repair stop time T_2. We ran computational simulations of the network model to validate the predicted optimal repair policies as interdependence is increased (*SI Appendix*, section S4). The results shown in Fig. 2*E* agree with the optimal policies calculated using Eq. **7** (solid lines).

Fluctuations in Failure Times. Using our framework, we have measured the extent of fluctuations in failure times with and without repair (Fig. 1*D*). The resulting distribution of failure times is described by the Weibull distribution (*SI Appendix*, section S3). Interestingly, we find that, in addition to increasing

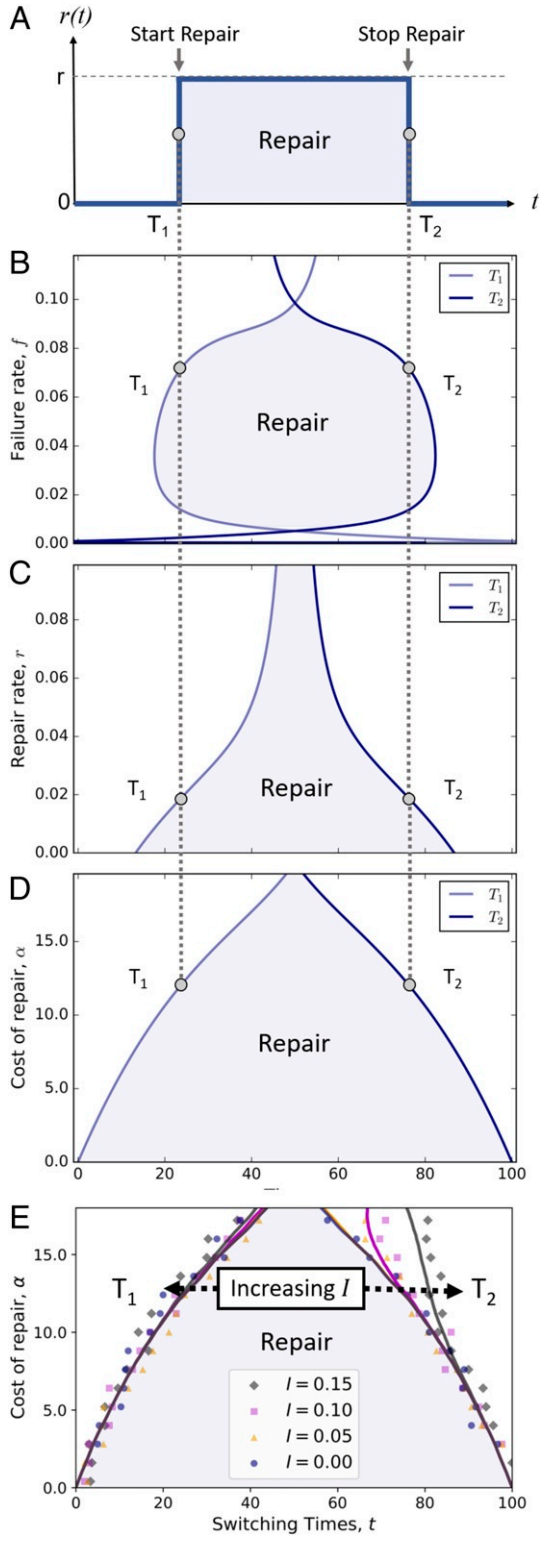

Fig. 2. Optimal repair protocols to maximize health span at minimum intervention cost. (*A*) Schematic representation of optimal bang-bang repair protocol $r(t)$ with repair start time T_1 and repair stop time T_2 as showcased in Eq. **8** for the linear regime. (*B*) The repair duration (shaded blue) is dependent on the failure rate f and disappears for small f and large f as calculated from Eq. **9**. (*C*) The repair duration monotonically decreases with increased maximum repair rate r. (*D*) The repair duration decreases with increased cost of repair α and disappears for large α. The default parameters used for *A–D* were $N = 1000$, $p = 0.1$, $f = 0.025$, $r = 0.01$, $\alpha = 10$, $\gamma = 0$, $T = 100$, $d = 0$, $I = 0$. (*E*) Optimal repair protocol for an interdependent network. Solid lines correspond to the numerical solution to the optimal control problem. Scatter points correspond to the optimal switching times obtained from a grid search on the computational model. The default parameters used were $N = 1000$, $p = 0.1$, $f = 0.025$, $r = 0.01$, $\gamma = 0$, $T = 100$, $d = 0$.

the average failure time, application of the finite horizon optimal repair protocol results in a broader distribution of network failure times (Fig. 1 *C–E*). This effect emerges naturally from the Weibull distribution, in which the mean failure time is linearly correlated with the SD in failure times for different values of f (Fig. 1*F*).

Role of Network Topology. We have also studied optimal protocols numerically for Erdős–Rényi $G(N, m)$ random networks (31) and Barabási–Albert scale-free networks (32). The aging dynamics are highly similar between the three network models investigated (*SI Appendix*, Fig. S6 *A–C*). For all random and scale-free networks, we observe no significant qualitative differences in the optimal repair protocols (*SI Appendix*, Fig. S6 *D* and *E*), indicating that our protocols are robust and may be applicable to a diverse range of complex systems.

A Generalization and an Application

Our computational and theoretical model of aging and its control in a complex network naturally raises the question of whether the optimal control policy that we determined can be iteratively learned and applied to a real system.

Reinforcement Learning Approach to Interdependent Network Aging Control. Optimal control strategies rely on knowledge of the model and a cost function, both of which are hard to crystallize into quantitative form in many biological systems. An alternative strategy is to ask whether the system is able to learn the optimal repair protocol for aging via an iterative procedure. This is tantamount to direct adaptive optimal control (36), embodied in reinforcement learning, a process by which a system is able to optimize its actions by interacting with its environment. Optimization occurs iteratively on a trial and error basis by reinforcing actions that maximize reward and/or minimize punishment. We use a relatively simple version of this algorithm known as Q learning (Fig. 3*A* and *SI Appendix*, Fig. S5) (29), which is a model-free alternative to dynamic programming models of the Bellman equation (37). This method consists of creating a Q matrix, $Q = \{\phi, r(\phi)\}$, which serves as a look-up table of vitality states ϕ and values associated with each possible action, $r(\phi) = 0$ or $r(\phi) = r$. In each training episode, a healthy $(d = 0)$ network is initialized. At each time step, the network is subjected to the aging algorithm, and the agent exploits network repair for the greatest-valued choice of repair at the given vitality of the system with probability $1 - e^{-\lambda_{\exp} q}$ where q is the number of episodes elapsed. The agent explores with probability $e^{-\lambda_{\exp} q}$. A reward R is calculated and used to update the state-action value in the Q matrix according to the rule (29)

$$Q(\phi_t, r_t) \leftarrow Q(\phi_t, r_t) + \beta\Big[R_t + \gamma_Q \max_{\rho}\{Q(\phi_{t+1}, \rho)\} - Q(\phi_t, r_t)\Big],$$

$$R_t = \phi_t - \alpha r_t,$$

where α is the cost of repair, β is the learning rate, and γ_Q is the Q-learning discount factor that is related to the optimal control through $\gamma = -\log \gamma_Q$. The learning rate exponentially decays as $\beta = e^{-\lambda_\beta q}$. An episode ends when the network fails (i.e., $\phi < 0.1$). The Q-learning model iterates through learning episodes

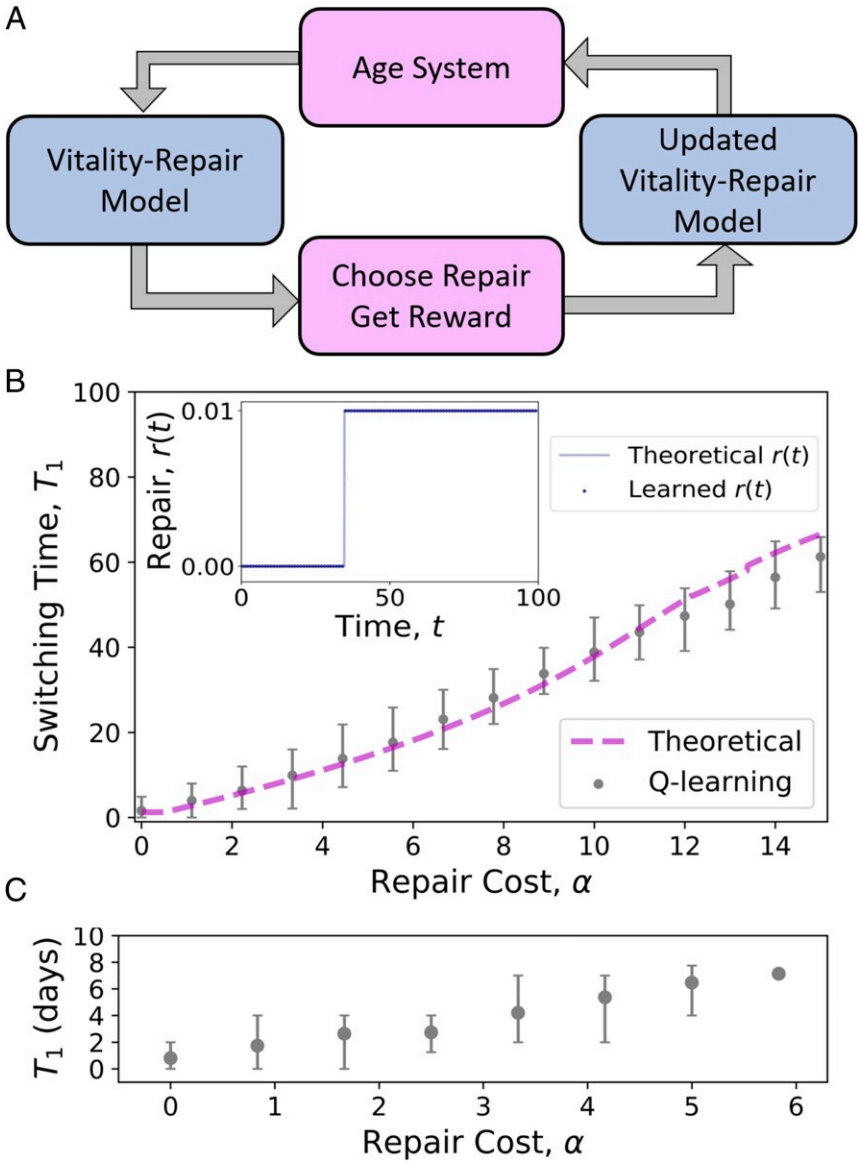

Fig. 3. Optimal repair protocols using reinforcement learning. (*A*) High-level schematic of reinforcement learning algorithm for optimal control of network aging. *SI Appendix*, section S5 has further *Q*-learning model details. (*B*) Optimal T_1 as a function of the cost of repair α for the reinforcement learning (gray circles; error bars span 75% CI, $N = 50$ realizations) and the theoretical solution (dotted magenta line) (Eq. **9**). Models used $N = 1000$, $p = 0.1$, $f = 0.025$, $r = 0.01$, $\gamma = 0.975$, $I = 0$. (*Inset*) The learned repair protocol (represented as points) is bang bang, matches closely with the theoretically optimal repair protocol (line) (Eq. **8**), and is characterized by a single repair switching time T_1. Parameters used were $f = 0.0367$, $r = 0.01$, $\alpha = 10$, $\gamma = 0.975$, $I = 0$, $d = 0$. (*C*) Switching time (in days) determined for α-ketoglutarate treatment of *C. elegans* (38) using estimated $f = 0.004$, $r = 0.043$, $I = 0.8$, and different choices of α. *Q* learning was used on network models ($N = 200$, $p = 0.1$). Error bars span 75% CI.

until qualitative convergence of the Q matrix is achieved. The optimal protocol is defined as the maximal Q-valued trajectory traveled by a network through (ϕ, r) space.

Using this method, the Q-learned repair policy converges to optimal repair protocols that are bang bang (Fig. 3*B*, *Inset*) and closely match the predicted switching time T_1 from the analytic theory for different values of α (Fig. 3*B*). These results suggest that the optimal protocols for repair can be obtained through simple iterative learning and highlight the potential of Q learning as a method to approximate optimal repair protocols for complicated systems in which no analytic description of the aging dynamics is available.

Quantifying the Protocols for Extending Longevity of *C. elegans*. We now deploy this approach using data from a model organism in aging research, the nematode *C. elegans*. We used *C. elegans* life span data (38–41) in the presence of a metabolite α-ketoglutarate that significantly extend *C. elegans* life span from which we estimate the parameters in our minimal model corresponding to the failure rate f, interdependency I, and α-ketoglutarate repair rate r (*SI Appendix*, section S7). Using Q learning with these fitted parameters, we predict optimal protocols for this system as a function of the cost of repair α (Fig. 3*C*). Consistent with our model, the switching time for α-ketoglutarate treatment increases with the cost of repair α. These results suggest that life-extending treatments that work through repair or replacement may be determined through measurable parameters. However, understanding the dependence of these strategies on the choice of the cost remains an outstanding question.

Discussion

Although aging in real biological and technological systems is a consequence of complex biochemical and mechanical processes, here we have abstracted a minimal model designed to capture the essential ingredients that give rise to aging in a complex system—modular units (nodes) that are linked to each other via a set of edges modeled as an interdependent network subject to nodal failure and repair. Our model shows the emergence of failure cascades, a hallmark of such systems, which we can understand using an analytic approach that accounts for both the observed mean and extreme value statistics of failure. We then deployed a simple scheme for repair in such interdependent systems, couched as an optimal control problem to slow down aging. We first used a model-dependent strategy to determine explicit optimal repair protocols for aging interdependent systems characterized by a failure rate f, repair rate r, and interdependency I. We also demonstrated that a model-free approach using reinforcement learning converges to these optimal repair protocols and can therefore be leveraged to approximate optimal repair strategies in an iterative manner. This allowed us to estimate model parameters for the efficacy of a drug used to increase the longevity of a model organism in aging studies—the nematode *C. elegans*.

We conclude with some implications of our work to the biological problem of determining optimal protocols for life-extending treatments such as the clearance of senescent cells. Senescent cells enter a permanent, nondividing state and adopt an altered secretory profile, which has been implicated in inflammation, tumorigenesis, and aging (10, 42). The presence of these cells has been shown to promote senescence in surrounding tissue (43), similar to how node failure in a network can spread due to interdependence. In contrast, the selective clearance of senescent cells (i.e., via the use of senolytic cocktails) improves physical function and survival (43, 44), without reducing either the total cell count (in human tissue) or body weight (in mouse models) (43). This suggests a rapid replacement of cleared senescent cells by healthy dividing cells, so that the application of senolytic treatments becomes analogous to node repair in an aging network. Like many life-extending compounds, senolytic cocktails may include toxicity (45, 46), which can be modeled in the cost function. The relative cost of repair α can be determined by separately measuring the loss of viability caused by senescence and the toxicity that results from treatment on an ensemble of healthy cells. This would allow for the deployment of our optimal repair protocols and design treatment schedules for senescent cell inhibitors and other therapeutics that target general aging processes.

Materials and Methods

There are no data associated with this paper.

ACKNOWLEDGMENTS. We acknowledge support from the Swiss National Science Foundation and the Amgen Scholars Program.

1. D. Harman, The aging process. *Proc. Natl. Acad. Sci. U.S.A.* **78**, 7124–7128 (1981).
2. Y. Bar-Yam, *Dynamics of Complex Systems* (Westview Press, 2003).
3. A. L. Barabási, Z. N. Oltvai, Network biology: Understanding the cell's functional organization. *Nat. Rev. Genet.* **5**, 101–113 (2004).
4. D. C. Vural, G. Morrison, L. Mahadevan, Aging in complex interdependency networks. *Phys. Rev.* **89**, 022811 (2014).
5. S. Taneja, A. B. Mitnitski, K. Rockwood, A. D. Rutenberg, Dynamical network model for age-related health deficits and mortality. *Phys. Rev. E* **93**, 022309 (2016).
6. S. G. Farrell, A. B. Mitnitski, K. Rockwood, A. D. Rutenberg, Network model of human aging: Frailty limits and information measures. *Phys. Rev. E* **94**, 052409 (2016).
7. A. B. Mitnitski, A. D. Rutenberg, S. Farrell, K. Rockwood, Aging, frailty and complex networks. *Biogerontology* **18**, 433–446 (2017).
8. N. Stroustrup *et al.*, The temporal scaling of *Caenorhabditis elegans* ageing. *Nature* **530**, 103–107 (2016).
9. N. Stroustrup, Measuring and modeling interventions in aging. *Curr. Opin. Cell Biol.* **55**, 129–138 (2018).
10. C. López-Otín, M. A. Blasco, L. Partridge, M. Serrano, G. Kroemer, The hallmarks of aging. *Cell* **153**, 1194–1217 (2013).
11. J. Gao, Y. Y. Liu, R. M. D'Souza, A. L. Barabási, Target control of complex networks. *Nat. Commun.* **5**, 5415 (2014).
12. Y. Y. Liu, J. J. Slotine, A. L. Barabási, Controllability of complex networks. *Nature* **473**, 167–173 (2011).
13. N. J. Cowan *et al.*, Nodal dynamics, not degree distributions, determine the structural controllability of complex networks. *PloS One* **7**, e38398 (2012).
14. L. Zhao, K. Park, Y. C. Lai, N. Ye, Tolerance of scale-free networks against attack-induced cascades. *Phys. Rev. E* **72**, 025104 (2005).
15. T. Tanizawa, G. Paul, R. Cohen, S. Havlin, H. E. Stanley, Optimization of network robustness to waves of targeted and random attacks. *Phys. Rev. E* **71**, 047101 (2005).
16. A. E. Motter, Cascade control and defense in complex networks. *Phys. Rev. Lett.* **93**, 098701 (2004).
17. W. X. Wang, G. Chen, Universal robustness characteristic of weighted networks against cascading failure. *Phys. Rev.* **77**, 026101 (2008).
18. B. Mirzasoleiman, M. Babaei, M. Jalili, M. Safari, Cascaded failures in weighted networks. *Phys. Rev. E* **84**, 046114 (2011).
19. D. I. Cho, M. Parlar, A survey of maintenance models for multi-unit systems. *Eur. J. Oper. Res.* **51**, 1–23 (1991).
20. L. C. Thomas, A survey of maintenance and replacement models for maintainability and reliability of multi-item systems. *Reliab. Eng.* **16**, 297–309 (1986).
21. W. P. Pierskalla, J. A. Voelker, A survey of maintenance models: The control and surveillance of deteriorating systems. *Nav. Res. Logist. Q.* **23**, 353–388 (1976).
22. H. Wang, A survey of maintenance policies of deteriorating systems. *Eur. J. Oper. Res.* **139**, 469–489 (2002).
23. R. Radner, D. W. Jorgenson, Opportunistic replacement of a single part in the presence of several monitored parts. *Manag. Sci.* **10**, 70–84 (1963).
24. R. E. Barlow, F. Proschan, *Mathematical Theory of Reliability* (SIAM, 1996).
25. Y. S. Sherif, M. L. Smith, Optimal maintenance models for systems subject to failure–A Review. *Nav. Res. Logist. Q.* **28**, 47–74 (1981).
26. S. M. Ross, A model in which component failure rates depend on the working set. *Nav. Res. Logist. Q.* **31**, 297–300 (1984).
27. H. Pham, H. Wang, Imperfect maintenance. *Eur. J. Oper. Res.* **94**, 425–438 (1996).
28. L. M. Hocking, *Optimal Control: An Introduction to the Theory with Applications* (Clarendon, 1991).
29. C. J. C. H. Watkins, P. Dayan, Q-learning. *Mach. Learn.* **8**, 279–292 (1992).
30. E. N. Gilbert, Random graphs. *Ann. Math. Stat.* **30**, 1141–1144 (1959).
31. Erdős P., Rényi A. (1960), On the evolution of random graphs. *Publ. Math. Inst. Hung. Acad. Sci.*, 45 (1960).
32. A. L. Barabási, R. Albert, Emergence of scaling in random networks. *Science* **286**, 509–512 (1999).
33. P. Crucitti, V. Latora, M. Marchiori, Model for cascading failures in complex networks. *Phys. Rev. E* **69**, 045104 (2004).
34. J. F. Fries, Aging, natural death, and the compression of morbidity. *Bull. World Health Organ.* **80**, 245–250 (2002).
35. T. B. L. Kirkwood, Understanding the odd science of aging. *Cell* **120**, 437–447 (2005).
36. R. Sutton, A. Barto, R. Williams, Reinforcement learning is direct adaptive optimal control. *IEEE Contr. Syst. Mag.* **12**, 19–22 (1992).
37. S. Bhasin, "Reinforcement learning and optimal control methods for uncertain nonlinear systems," PhD dissertation, Department of Mechanical and Aerospace Engineering, University of Florida, Gainesville, FL (2011).
38. R. M. Chin *et al.*, The metabolite α-ketoglutarate extends lifespan by inhibiting ATP synthase and TOR. *Nature* **510**, 397–401 (2014).
39. 39.G. D. Lee *et al.*, Dietary deprivation extends lifespan in *Caenorhabditis elegans*. *Aging Cell* **5**, 515–524 (2006).
40. I. Alfaras *et al.*, Health benefits of late-onset metformin treatment every other week in mice. *NPJ Aging Mech. Dis.* **3**, 16 (2017).
41. D. E. Harrison *et al.*, Rapamycin fed late in life extends lifespan in genetically heterogeneous mice. *Nature* **460**, 392–395 (2009).
42. J. Campisi, F. d'Adda di Fagagna, Cellular senescence: When bad things happen to good cells. *Nat. Rev. Mol. Cell Biol.* **8**, 729–740 (2007).
43. M. Xu *et al.*, Senolytics improve physical function and increase lifespan in old age. *Nat. Med.* **24**, 1246–1256 (2018).
44. D. J. Baker *et al.*, Clearance of $p16^{ink4a}$-positive senescent cells delays ageing-associated disorders. *Nature* **479**, 232–236 (2011).
45. M. Serrano, N. Barzilai, Targeting senescence. *Nat. Med.* **24**, 1092–1094 (2018).
46. J. L. Kirkland, T. Tchkonia, Cellular senescence: A translational perspective. *EBioMedicine* **21**, 21–28 (2017).

PNAS
www.pnas.org

Supplementary Information for

Optimal control of aging in complex networks

Eric D. Sun, Thomas C.T. Michaels and L. Mahadevan

L. Mahadevan.
E-mail: lmahadev@g.harvard.edu

This PDF file includes:

Contents

Supporting Information Text

S1. Analytic framework

S1.1. Aging dynamics in interdependent networks. The dynamical equation that describes the evolution of the mean network vitality Φ with time can be formulated as function of three relevant physical parameters:

- the failure rate f,
- repair rate r, and
- interdependency I.

The total rate of change of vitality is the sum of the rates of node failure and repair; we now derive these two terms by accounting for interdependence between the components.

S1.1.1. Network failure. For network failure, a node can either fail with probability f or when its vital fraction falls below I. Thus, the total rate of failure f_{tot} is set by two contributions. To capture the role of interdependence between the components at the network level, it is useful to consider the fraction of nodes that have one remaining vital provider over the threshold I, which we denote as $m(I, \Phi)$. We can estimate $m(I, \Phi)$ in the mean-field limit. Assume that each node is connected to z nodes on average; then $m(I, \Phi)$ is equal to the probability that $k = zI$ of these nodes is alive, while the remaining $z - k$ nodes are failed. The probability that a node is alive is Φ, hence (Fig. S1(b))

$$m(I, \Phi) = \binom{z}{k} \Phi^k (1 - \Phi)^{z-k} \quad [S1]$$

Vural et. al. (1) proposed the following recurrence relation to describe the effective failure rate f_{tot}:

$$f_{\text{tot}} = f + m(I = 0.5, \Phi) f_{\text{tot}} (1 - f) \quad [S2]$$

This relation must be modified to reproduce the vitality collapse in the network. First, the susceptible fraction $m(I, \Phi)$ should be calculated with respect to the population of live nodes rather than the entire network resulting in $m(I, \Phi)/\Phi$. This modification is needed because the possibility of node failure is conditioned on a node being alive. Secondly, Eq. (S2) considers a single target vital provider. However, when $I > 1/N$ (where N is the number of nodes in the network) then susceptible nodes will have more than one vital provider. Therefore, the probability of a final vital provider failing is the probability of at least one of $k = zI$ vital providers failing (rather than a target provider failing as in Eq. (S2)). This probability is $1 - (1 - f_{\text{tot}})^k$. Thus, the recurrence relation is modified to

$$f_{\text{tot}} = f + m(I, \Phi)(1 - (1 - f_{\text{tot}})^k)(1 - f) \quad [S3]$$

For small failure rate f, a first-order binomial expansion results in $(1 - f_{\text{tot}})^k \simeq 1 - k f_{\text{tot}}$ and therefore

$$f_{\text{tot}} \simeq f + m(I, \Phi) k f_{\text{tot}} (1 - f). \quad [S4]$$

Solving the recurrence relation results in the effective failure rate

$$f_{\text{tot}} = \frac{f}{1 - k(1 - f) m(I, \Phi)}, \quad [S5]$$

and this gives the failure term for the average network vitality Φ

$$\left.\frac{d\Phi}{dt}\right|_f = -\frac{f}{1 - k(1 - f) m(I, \Phi)} \Phi, \quad [S6]$$

S1.1.2. Network repair. For network repair, a failed node can be successfully repaired with probability r but would be conditioned for immediate failure if the vital fraction of its neighbors is less than the threshold I. As a result, the effective repair experienced by the network is less than or equal to r. In the mean field, this implies that the effective repair rate is $r_{\text{tot}} = r\, h(I, \Phi)$, where $h(I, \Phi)$ is the average fraction of nodes that have a vital fraction greater than I (Fig. S1(a))

$$h(I, \Phi) = \sum_{j=k}^{z} \binom{z}{j} \Phi^j (1 - \Phi)^{z-j}, \quad [S7]$$

where $k = zI$. Therefore, the repair term for the average network vitality Φ is

$$\left.\frac{d\Phi}{dt}\right|_r = r\, h(I, \Phi)(1 - \Phi), \quad [S8]$$

where $1 - \Phi$ is the fraction of failed nodes.

S1.1.3. Full dynamic equation. Combining Eq. (S6) and Eq. (S8) leads to the full dynamical description of network aging:

$$\frac{d\Phi}{dt} = \left.\frac{d\Phi}{dt}\right|_f + \left.\frac{d\Phi}{dt}\right|_r = -\frac{f\Phi}{1 - k(1 - f) m(I, \Phi)} + r\, h(I, \Phi)(1 - \Phi). \quad [S9]$$

Representative examples for the time evolution of vitality described by Eq. (S9) are shown in Fig. S1(c). The system vitality decreases exponentially with time initially; as the vitality approaches a threshold Φ_c, the total failure rate becomes large, leading to failure cascade and a rapid decrease of vitality. This critical vitality can be estimated by maximising $m(I, \Phi)$ over Φ, leading to

$$\Phi_c \simeq I. \quad [S10]$$

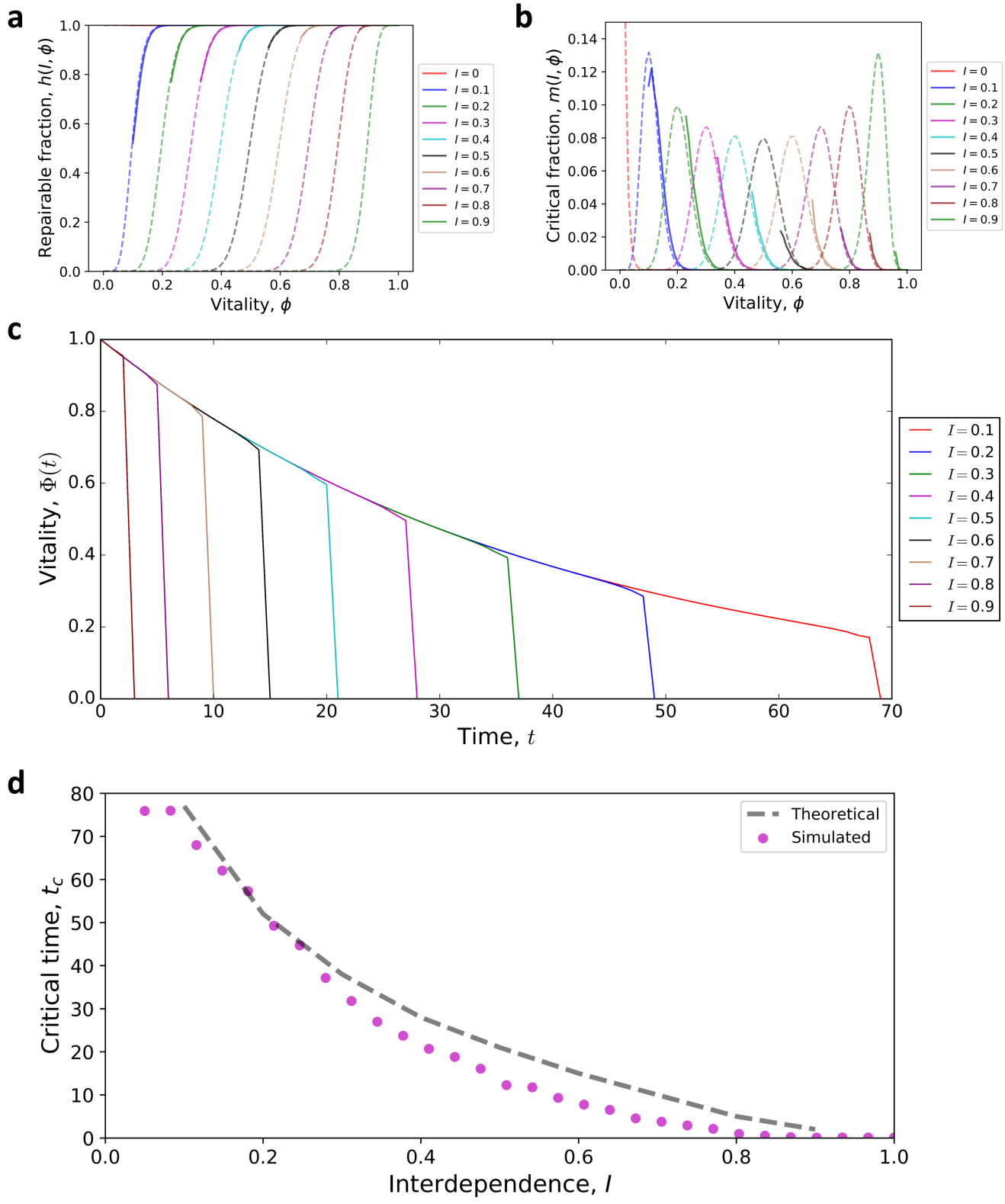

Fig. S1. Computational validation of the analytic theory. (a) $h(I, \Phi)$ for different values of I. (b) $m(I, \Phi)$ for different values of I. Solid curves correspond to simulated results from the computational model and dotted curves correspond to the analytic approximation. Simulated results were averaged for 100 Gilbert random networks with $N = 1000$. (c) Numerical solutions to the nonlinear interdependent model of aging for different values of I. (d) Simulated times for collapse (defined as $\Phi(t_c) = \Phi_c$) are compared to theoretical prediction from Eq. (S10) (solid line). Calculation parameters: $f = 0.025$, $r = 0.01$, $\alpha = 10$, $d = 0$, $\gamma = 0$.

S2. Optimal control theory of aging in an interdependent network

S2.1. Definition of optimal control problem. We can start by considering the aging dynamics of the mean-field network vitality Φ, Eq. (6) of the main text, and make the repair rate time dependent, i.e. set $r = r(t)$. Then, the system dynamics is given by

$$\frac{d\Phi}{dt} = -f_{\rm tot}\Phi + r_{\rm tot}(1-\Phi), \tag{S11}$$

where $f_{\rm tot}$ and $r_{\rm tot}$ are the total rates of failure and repair, given by

$$f_{\rm tot} = \frac{f}{1 - km(I,\Phi)(1-f)}, \tag{S12}$$

$$r_{\rm tot} = rh(I,\Phi). \tag{S13}$$

Here f and r are the intrinsic rates of failure and repair and

$$m(I,\Phi) = \binom{z}{k}\Phi^k(1-\Phi)^{z-k} \tag{S14}$$

$$h(I,\Phi) = \sum_{j=k}^{z}\binom{z}{j}\Phi^j(1-\Phi)^{z-j} \tag{S15}$$

are the probabilities that a node has k, respectively, more than k vital providers, where $k = zI$. Note that in the limit of no interdependence, corresponding to $I = 0$, we have $h(I=0,\Phi) = 1$ and $f_{\rm tot} = f$. In this case, we obtain a linear equation for vitality

$$\frac{d\Phi}{dt} = -f\Phi + r(1-\Phi). \tag{S16}$$

As discussed in the main text, the control variable in the problem is $r(t)$ (the repair protocol) and the goal of the optimal control problem is to determine $r(t)$ such that the cost is minimized

$$\text{Cost} = \int_0^T e^{-\gamma t}\Big[\alpha r(t) - \Phi(t)\Big]dt, \tag{S17}$$

where γ is the discount rate and α is the relative cost of repair.

S2.2. Solution to optimal control problem. We solve the optimal control problem given by Eq. (S11) and Eq. (S17) with the framework of optimal control theory (Pontryagin's minimum principle) (2). Due to the presence of the discount factor $e^{-\gamma t}$ in Eq. (S17), we can solve the optimal control problem by introducing the so-called current Hamiltonian*

$$\mathcal{H} = \alpha r - \Phi + \lambda\Big[r_{\rm tot}(1-\Phi) - f_{\rm tot}\Phi\Big], \tag{S18}$$

where $\lambda(t)$ is a co-state variable. The optimal protocol is determined by minimizing $\mathcal{H}$ with respect to the control r, yielding

$$\frac{\partial\mathcal{H}}{\partial r} = 0 \quad \Rightarrow \quad \alpha + \lambda\, h\,(1-\Phi) = 0 \tag{S19}$$

---

*An alternative approach to the current Hamiltonian formalism is to introduce the following Hamiltonian (obtained directly by considering the full integrand of the cost, while the current Hamiltonian has no $e^{-\gamma t}$ term):

$$\mathcal{H}_0 = e^{-\gamma t}\Big[\alpha r - \Phi\Big] + \lambda_0\Big[r_{\rm tot}(1-\Phi) - f_{\rm tot}\Phi\Big],$$

where λ_0 is the co-state variable associated with the Hamiltonian $\mathcal{H}_0$ (note that λ_0 is not the same as λ). Pontryagin's minimum principle applied to $\mathcal{H}_0$ implies

$$\begin{aligned}
0 &= \frac{\partial\mathcal{H}_0}{\partial r} = e^{-\gamma t}\alpha + \lambda_0\, h\,(1-\Phi)\\
\frac{d\Phi}{dt} &= \frac{\partial\mathcal{H}_0}{\partial\lambda_0} = -f_{\rm tot}\Phi + r_{\rm tot}(1-\Phi)\\
\frac{d\lambda_0}{dt} &= -\frac{\partial\mathcal{H}_0}{\partial\Phi} = e^{-\gamma t} + \lambda_0\,(f_{\rm tot} + r_{\rm tot}) + \lambda_0\,\Phi\,\frac{\partial f_{\rm tot}}{\partial\Phi} - \lambda_0(1-\Phi)\,\frac{\partial r_{\rm tot}}{\partial\Phi},
\end{aligned}$$

with $\lambda_0(T) = 0$. This calculation with $\mathcal{H}_0$ is equivalent to that using the current Hamiltonian, Eq. (S18). This can be seen by writing $\lambda = e^{\gamma t}\lambda_0$ yielding:

$$\begin{aligned}
0 = e^{-\gamma t}\Big[\alpha + \lambda\, h\,(1-\Phi)\Big] \quad &\Rightarrow \quad 0 = \alpha + \lambda\, h\,(1-\Phi) = \frac{\partial\mathcal{H}}{\partial r}\\
\frac{d\Phi}{dt} &= -f_{\rm tot}\Phi + r_{\rm tot}(1-\Phi)\\
\frac{d\lambda}{dt} = \gamma\lambda + e^{\gamma t}\frac{d\lambda_0}{dt} &= \gamma\lambda + 1 + \lambda\,(f_{\rm tot} + r_{\rm tot}) + \lambda\,\Phi\,\frac{\partial f_{\rm tot}}{\partial\Phi} - \lambda(1-\Phi)\,\frac{\partial r_{\rm tot}}{\partial\Phi} = \gamma\lambda - \frac{\partial\mathcal{H}}{\partial\Phi},
\end{aligned}$$

with $\lambda(T) = e^{\gamma T}\lambda_0(T) = 0$. This is equivalent to Eq. (S19), Eq. (S22), and Eq. (S23). Thus $\mathcal{H}_0$ and the current Hamiltonian $\mathcal{H}$ yield the same results.

The optimal control is thus a bang-bang control that switches between $r(t) = 0$ and $r(t) = r$ depending on the sign of the function $\alpha + \lambda\, h\,(1 - \Phi)$ (this is known as switching function). In particular, if $\alpha + \lambda\, h\,(1 - \Phi) > 0$, we have $r(t) = 0$, while if $\alpha + \lambda\, h\,(1 - \Phi) < 0$, we have $r(t) = r$. Noticing that $\lambda(t)$ is negative,[†] the optimal repair protocol reads

$$r(t) = \begin{cases} r, & h\,(1-\Phi) > \alpha/|\lambda| \\ 0, & h\,(1-\Phi) < \alpha/|\lambda| \end{cases} \qquad [S20]$$

which is Eq. (7) of the main text. The number of switches in the optimal protocol is determined by the number of zeros of the switching function

$$\alpha + \lambda\, h\,(1 - \Phi). \qquad [S21]$$

The solution to the optimal control problem, Eq. (S20), states that the repair rate is switched on when the repairable fraction of nodes, $h(I, \Phi)(1 - \Phi)$, exceeds a time-dependent threshold given by α/λ. The repairable fraction increases with time as nodes in the network fail and/or become increasingly susceptible to failure cascades; on the other hand, the threshold for the repairable fraction also increases with time as the system ages, leading to a smaller window of repair.

To find the times when $r(t)$ equals 0 or r, we thus need to solve for the functions λ and Φ. The dynamic equations for these two variables are obtained directly from the Hamiltonian Eq. (S18). The equation for Φ is

$$\frac{d\Phi}{dt} = \frac{\partial \mathcal{H}}{\partial \lambda} = -f_{\rm tot}\Phi + r_{\rm tot}(1 - \Phi), \qquad [S22]$$

with initial condition $\Phi(0) = 1 - d$. The equation for λ is

$$\frac{d\lambda}{dt} = \gamma\lambda - \frac{\partial \mathcal{H}}{\partial \Phi} = 1 + (\gamma + f_{\rm tot} + r_{\rm tot})\lambda + \lambda\,\Phi\,\frac{\partial f_{\rm tot}}{\partial \Phi} - \lambda(1 - \Phi)\,\frac{\partial r_{\rm tot}}{\partial \Phi}, \qquad [S23]$$

with the boundary condition $\lambda(T) = 0$ (this condition is referred to as the terminal condition).

S2.3. Linearized control problem. We now discuss the linearized limit of Eq. (S11), when explicit analytical expressions for the optimal protocol can be obtained. In this case, condition Eq. (S20) yield non-monotonic optimal repair protocols characterized by a waiting time for repair, followed by an intermediate period where repair is preferred and a terminal phase where the repair rate is set again to zero. This optimal protocol can be written as

$$r(t) = \begin{cases} 0, & t < T_1 \\ r, & T_1 < t < T_2 \\ 0, & t > T_2 \end{cases} \qquad [S24]$$

where T_1 and T_2 are the switching times, which we determine here below using the switching function Eq. (S21). In the linearized limit, the dynamic equation for Φ, Eq. (S22), reduces to

$$\frac{d\Phi}{dt} = r - (f + r)\Phi, \qquad [S25]$$

while the equation for λ, Eq. (S23), becomes

$$\frac{d\lambda}{dt} = 1 + (\gamma + f + r)\lambda. \qquad [S26]$$

For $t < T_1$ and $t \geq T_2$, we have $r(t) = 0$, while for $T_1 \leq t < T_2$ we have $r(t) = r$; thus, the solution to Eq. (S25) for Φ is given

$$\Phi(t) = \begin{cases} (1-d)e^{-ft}, & t < T_1 \\ \Phi(T_1)e^{-(r+f)(t-T_1)} + \frac{r(1-e^{-(r+f)(t-T_1)})}{r+f}, & T_1 < t < T_2 \\ \Phi(T_2)e^{-f(t-T_2)} & T_2 < t \end{cases} \qquad [S27]$$

[†] Note that the function λ is always ≤ 0 on $t \in [0, T]$. This can be shown by solving Eq. (S23). This equation can be written in the form

$$\frac{d\lambda}{dt} = 1 + g(t)\,\lambda(t),$$

where $g = \gamma + f_{\rm tot} + r_{\rm tot} + \Phi\,\frac{\partial f_{\rm tot}}{\partial \Phi} - (1 - \Phi)\,\frac{\partial r_{\rm tot}}{\partial \Phi}$. The solution subject to $\lambda(T) = 0$ is

$$\lambda(t) = \int_T^t e^{G(t)-G(s)}ds, \quad \text{where } G(t) = \int_T^t g(s)ds.$$

Since the integrand $e^{G(t)-G(s)} > 0$, it follows that

$$\lambda(t) = -\int_t^T e^{G(t)-G(s)}ds \leq 0.$$

Similarly, the solution to Eq. (S26) for λ can be constructed piecewise from the transversality condition $\lambda(T) = 0$ as

$$\lambda(t) = \begin{cases} \lambda(T_1)e^{(f+\gamma)(t-T_1)} + \frac{e^{(f+\gamma)(t-T_1)}-1}{f+\gamma}, & t < T_1 \\ \lambda(T_2)e^{(r+f+\gamma)(t-T_2)} + \frac{e^{(r+f+\gamma)(t-T_2)}-1}{f+r+\gamma}, & T_1 < t < T_2 \\ \frac{e^{(f+\gamma)(t-T)}-1}{f+\gamma} & T_2 < t \end{cases} \quad [S28]$$

Having determined the time evolution of the functions Φ and λ (see Fig. S2), we are now in position to determine the switching times T_1 and T_2 for the optimal bang-bang control. Note that $|\lambda|$ decreases with time (λ is negative), while $1 - \Phi$ increases with time. Hence, the product $(\Phi - 1)\lambda$ is a positive, non-monotonic function of time. The crossing points with the line α correspond to the switching times T_1 and T_2 (Fig. S2(d)). These are determined as solutions to the following equation

$$\left[\Phi(T_i) - 1\right] \lambda(T_i) = \alpha, \quad i = 1, 2. \quad [S29]$$

Thus

$$\left[(1-d)e^{-fT_1} - 1\right] \cdot \left[\frac{e^{(f+\gamma)(T_2-T)} - 1}{f+\gamma} e^{(r+f+\gamma)(T_1-T_2)} + \frac{e^{(r+f+\gamma)(T_1-T_2)} - 1}{f+r+\gamma}\right] = \alpha \quad [S30a]$$

$$\left[(1-d)e^{-fT_1}e^{-(r+f)(T_2-T_1)} + \frac{r(1-e^{-(r+f)(T_2-T_1)})}{r+f} - 1\right] \cdot \left[\frac{e^{(f+\gamma)(T_2-T)} - 1}{f+\gamma}\right] = \alpha \quad [S30b]$$

We can solve these equations using the following approximations: for calculating T_1, we use $\lambda \simeq -1/(\gamma + r + f)$; when calculating T_2, we use $\Phi - 1 \simeq -f/(r + f)$. Thus, we arrive at

$$\left[1 - (1-d)e^{-fT_1}\right] = \alpha(r + f + \gamma) \quad [S31]$$

$$\left[1 - e^{(f+\gamma)(T_2-T)}\right] = \frac{\alpha(r+f)(f+\gamma)}{f}. \quad [S32]$$

The solution is

$$T_1 \simeq \frac{1}{f} \log\left[\frac{1-d}{1-\alpha(f+r+\gamma)}\right] \quad [S33]$$

$$T_2 \simeq T - \frac{1}{f+\gamma} \log\left[\frac{1}{1-\alpha(f+r)(f+\gamma)/f}\right], \quad [S34]$$

which is Eq. (9) of the main text.

S2.3.1. Curvature around optimum. We now compute the cost as the repair protocol deviates from the optimum:

$$r(t) = \begin{cases} 0, & t < T_1 \\ r, & T_1 < t < T_2 \\ 0, & t > T_2 \end{cases} \quad [S35]$$

where T_1 and T_2 now denote arbitrary switching times, not necessarily the optimal values. The cost for repair is

$$\text{Cost}_r = \int_0^T e^{-\gamma t}\alpha r(t)dt = \alpha r \int_{T_1}^{T_2} e^{-\gamma t}dt = \frac{\alpha r}{\gamma}\left(e^{-\gamma T_1} - e^{-\gamma T_2}\right). \quad [S36]$$

The cost associated with vitality is estimated using the analytical solution Eq. (S27) as

$$\text{Cost}_\phi = -\int_0^T e^{-\gamma t}\Phi(t)dt = -\int_0^{T_1} e^{-\gamma t}\Phi(t)dt - \int_{T_1}^{T_2} e^{-\gamma t}\Phi(t)dt - \int_{T_2}^{T} e^{-\gamma t}\Phi(t)dt, \quad [S37a]$$

where

$$\int_0^{T_1} e^{-\gamma t}\Phi(t)dt = \frac{1}{\gamma + f}\left(\Phi(0) - \Phi(T_1)e^{-\gamma T_1}\right), \quad [S37b]$$

$$\int_{T_1}^{T_2} e^{-\gamma t}\Phi(t)dt = e^{-\gamma T_1}\left[\frac{r}{\gamma(r+f)}\left(1 - e^{-\gamma(T_2-T_1)}\right) + \left(\Phi(T_1) - \frac{r}{r+f}\right)\frac{1 - e^{-(r+f+\gamma)(T_2-T_1)}}{r+f+\gamma}\right], \quad [S37c]$$

$$\int_{T_2}^{T} e^{-\gamma t}\Phi(t)dt = \frac{\Phi(T_2)e^{-\gamma T_2}}{\gamma + f}\left(1 - e^{-(f+\gamma)(T-T_2)}\right). \quad [S37d]$$

The total cost

$$\text{Cost} = \int_0^T e^{-\gamma t}\big[\alpha r(t) - \Phi(t)\big]\,dt \tag{S38}$$

is then obtained by combining Eq. (S36) and Eq. (S37) yielding:

$$\begin{aligned}\text{Cost} = &\frac{r}{\gamma(r+f)}\left(\alpha(r+f)-1\right)\left(e^{-\gamma T_1}-e^{-\gamma T_2}\right) - \frac{1-d}{f+\gamma}\left(1-e^{-(f+\gamma)T_1}\right) \\ &+ \frac{r-(r+f)\Phi(T_1)}{(r+f+\gamma)(r+f)}e^{-\gamma T_1}\left(1-e^{-(f+r+\gamma)(T_2-T_1)}\right) - \frac{\Phi(T_2)}{f+\gamma}e^{-\gamma T_2}\left(1-e^{-(f+\gamma)(T-T_2)}\right).\end{aligned} \tag{S39}$$

The total cost is shown in Fig. S2(e) as a function of T_1 and T_2. It has a distinct minimum in correspondence of the optimal switching times T_1 and T_2. We can determine this optimal protocol explicitly by minimizing the cost with respect to T_1 and T_2. Using the approximation $e^{-(r+f+\gamma)(T_2-T_1)}, e^{-(r+f)(T_2-T_1)} \ll 1$, we obtain

$$\begin{aligned}\text{Cost} \simeq &\frac{r}{\gamma(r+f)}\left(\alpha(r+f)-1\right)\left(e^{-\gamma T_1}-e^{-\gamma T_2}\right) - \frac{1-d}{f+\gamma}\left(1-e^{-(f+\gamma)T_1}\right) \\ &+ \frac{r-(r+f)(1-d)e^{-fT_1}}{(r+f+\gamma)(r+f)}e^{-\gamma T_1} - \frac{r}{(r+f)(f+\gamma)}e^{-\gamma T_2}\left(1-e^{-(f+\gamma)(T-T_2)}\right),\end{aligned} \tag{S40}$$

and therefore

$$\frac{\partial \text{Cost}}{\partial T_1} = 0 \quad \Rightarrow \quad T_1 \simeq \frac{1}{f}\log\left[\frac{1-d}{1-\alpha(f+r+\gamma)}\right], \tag{S41a}$$

$$\frac{\partial \text{Cost}}{\partial T_2} = 0 \quad \Rightarrow \quad T_2 \simeq T - \frac{1}{f+\gamma}\log\left[\frac{1}{1-\alpha(f+r)(f+\gamma)/f}\right], \tag{S41b}$$

which is the same as Eq. (S33) and Eq. (S34). The cost function Eq. (S40) thus has one single minimum point. We now verify that this is indeed a minimum of the cost. To this end we evaluate the Hessian matrix at the optimum. In the limit $\gamma = 0$ we find

$$\text{Hess}(T_1^\star, T_2^\star) = \left.\begin{pmatrix} \frac{\partial^2 \text{Cost}}{\partial T_1^2} & \frac{\partial^2 \text{Cost}}{\partial T_1 \partial T_2} \\ \frac{\partial^2 \text{Cost}}{\partial T_1 \partial T_2} & \frac{\partial^2 \text{Cost}}{\partial T_2^2} \end{pmatrix}\right|_{T_1=T_1^\star, T_2=T_2^\star} = \frac{fr\left[1-\alpha(f+r)\right]}{f+r}\begin{pmatrix} 1 & 0 \\ 0 & 1 \end{pmatrix}. \tag{S42}$$

Since $\alpha(f+r) < 1$, the Hessian Eq. (S42) is positive definite and Eq. (S41) is a global minimum of the cost Eq. (S40). The curvature around the optimum is thus given by

$$\kappa = \frac{fr\left[1-\alpha(f+r)\right]}{f+r}. \tag{S43}$$

S2.3.2. Life time increase. We now investigate how life time increases when an optimal repair protocol is applied in the linear regime and in the infinite horizon limit. Life time is defined through the condition $\Phi(T_{\text{life}}) = \Phi_c$, where Φ_c is a critical vitality value. In the absence of repair, the life time is given by:

$$T_{\text{life}} = \frac{1}{f}\log\left(\frac{1}{\Phi_c}\right). \tag{S44}$$

If an optimal repair protocol is applied, the expected life time becomes (see Fig. S3):

$$T_{\text{life}} = \begin{cases} \frac{1}{f}\log\left(\frac{1}{\Phi_c}\right) & \alpha(r+f+\gamma) < 1-\Phi_c \\ T_1 + \frac{1}{f+r}\log\left(\frac{f-\alpha(f+r)(f+r+\gamma)}{(f+r)\Phi_c - r}\right) & \alpha(r+f+\gamma) > 1-\Phi_c \end{cases} \tag{S45}$$

S2.3.3. Connection to Hamilton-Jacobi-Bellman equation. We now derive optimal repair protocols using the Hamilton-Jacobi-Bellman (HJB) equation. We are looking for a function $V : [0,T] \times [0,1] \to \mathbb{R}$ (Bellman value function) which satisfies the HJB equation

$$\frac{\partial V}{\partial t} + \min_r\left(\alpha\, r - \Phi + [r-(f+r)\Phi]\frac{\partial V}{\partial \Phi}\right) = 0. \tag{S46}$$

We can rewrite the HJB equation as

$$\frac{\partial V}{\partial t} - \Phi - f\,\Phi\,\frac{\partial V}{\partial \Phi} + \min_r r\left(\alpha + (1-\Phi)\frac{\partial V}{\partial \Phi}\right) = 0. \tag{S47}$$

The minimum depends clearly on the sign of the function $\alpha + (1-\Phi)\partial V/\partial\Phi$. In particular,

$$r(t) = \begin{cases} 0, & \alpha + (1-\Phi)\frac{\partial V}{\partial \Phi} > 0 \\ r, & \alpha + (1-\Phi)\frac{\partial V}{\partial \Phi} < 0 \end{cases} \tag{S48}$$

We consider both cases separately.

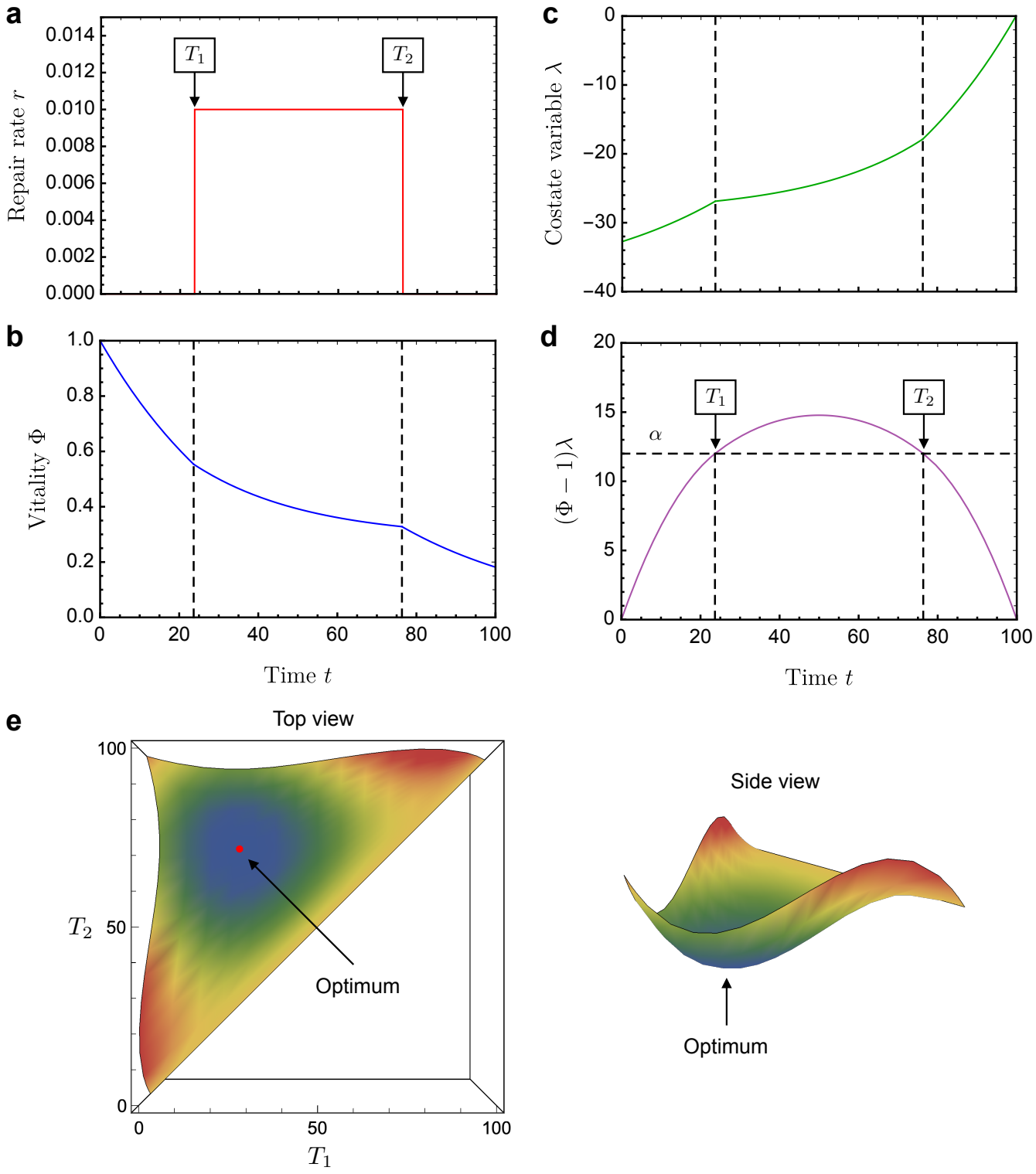

Fig. S2. Optimal control for linear theory. (a) Optimal repair protocol $r(t)$ with switching times T_1 and T_2. (b) Vitality Φ as a function of time. (c) Costate variable λ as a function of time. (d) The function $(\Phi-1)\lambda$ is non-monotonic with time. The crossing points with α correspond to the switching times. (e) Total cost is plotted as a function of T_1 and T_2 shows a distinct minimum in correspondence of optimal switching times. Calculation parameters: $f=0.025$, $r=0.01$, $\alpha=12$, $T=100$, $d=0$, $\gamma=0$.

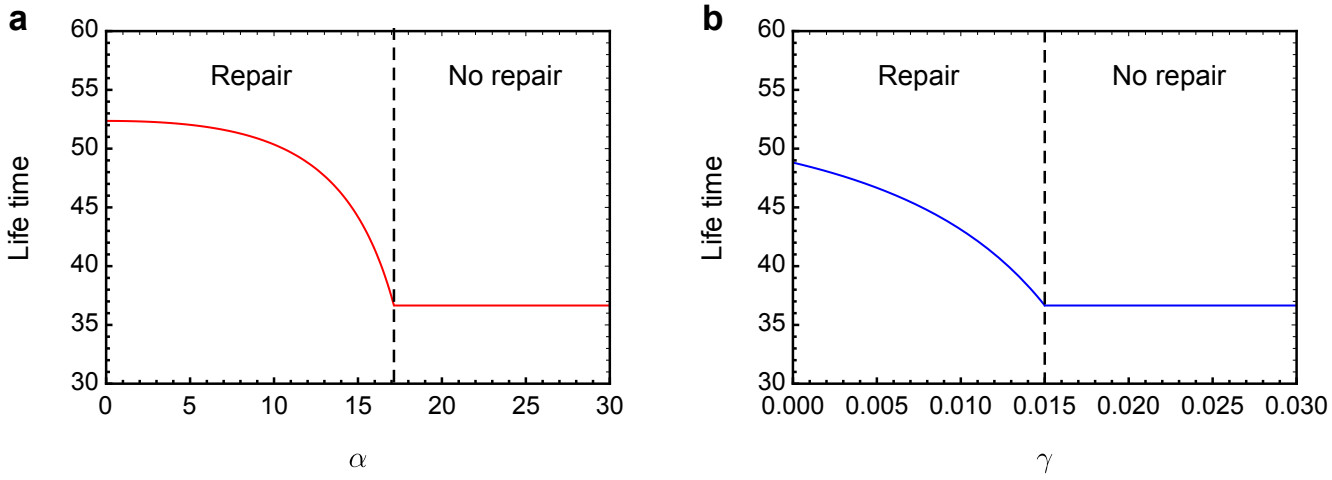

Fig. S3. Life time increase. Life time $T_{\rm life}$ under optimal repair conditions as a function of α (a) and γ (b). Calculation parameters: $f = 0.025$, $r = 0.01$, $\alpha = 12$, $T = \infty$, $d = 0$, $\gamma = 0$, $\Phi_c = 0.4$.

- When $r(t) = 0$, the HJB equation becomes

$$\frac{\partial V}{\partial t} - \Phi - f\,\Phi\,\frac{\partial V}{\partial \Phi} = 0. \tag{S49}$$

The solution subject to $V(T, \Phi) = 0$ ($\Rightarrow \partial V(T, \Phi)/\partial\Phi = 0$) is

$$V(t, \Phi) = \Phi\,\frac{e^{f(t-T)} - 1}{f}. \tag{S50}$$

- When $r(t) = r$, the HJB equation becomes

$$\frac{\partial V}{\partial t} - \Phi - f\,\Phi\,\frac{\partial V}{\partial \Phi} + r\left(\alpha + (1-\Phi)\frac{\partial V}{\partial \Phi}\right) = 0. \tag{S51}$$

The solution is

$$V(t, \Phi) = -\frac{\Phi}{r+f} + \frac{rt[1-\alpha(r+f)]}{r+f} + d\left(\Phi - \frac{r}{r+f}\right)e^{(f+r)t}. \tag{S52}$$

By matching Eq. (S50) and Eq. (S52) at $t = T_2$, we find:

$$V(t, \Phi) = -\frac{\Phi}{r+f} + \frac{rt[1-\alpha(r+f)]}{r+f} + e^{-(f+r)T_2}\left(\frac{e^{f(T_2-T)}-1}{f} + \frac{1}{f+r}\right)\left(\Phi - \frac{r}{r+f}\right)e^{(f+r)t}. \tag{S53}$$

In summary the Bellman value function is:

$$V(t, \Phi) = \begin{cases} \Phi\,\frac{e^{f(t-T)}-1}{f} & T_2 < t < T \\ -\frac{\Phi}{r+f} + \frac{rt[1-\alpha(r+f)]}{r+f} + e^{-(f+r)T_2}\left(\frac{e^{f(T_2-T)}-1}{f} + \frac{1}{f+r}\right)\left(\Phi - \frac{r}{r+f}\right)e^{(f+r)t} & T_1 < t < T_2 \end{cases} \tag{S54}$$

To obtain the switching times, we impose the condition $\alpha + (1-\Phi)\partial V/\partial\Phi = 0$ at $t = T_1, T_2$:

$$t = T_1: \qquad \alpha + \big[1 - \Phi(T_1)\big]\left[\frac{e^{f(T_2-T)}-1}{f}e^{(r+f)(T_1-T_2)} + \frac{e^{(r+f)(T_1-T_2)}-1}{f+r}\right] = 0 \tag{S55a}$$

$$t = T_2: \qquad \alpha + \big[1 - \Phi(T_2)\big]\left[\frac{e^{f(T_2-T)}-1}{f}\right] = 0. \tag{S55b}$$

This is equivalent to Eq. (S30).

S2.4. Singular arcs. According to Pontryagin's minimum principle, the optimal repair protocol is determined by the condition $\partial\mathcal{H}/\partial r = 0$ (see Eq. (S19)) yielding

$$r(t) = \begin{cases} r, & h\,(1-\Phi) > \alpha/|\lambda| \\ 0, & h\,(1-\Phi) < \alpha/|\lambda| \end{cases} \tag{S56}$$

It is however not clear what happens when $h\,(1-\Phi) = \alpha/|\lambda|$, where Pontryagin's minimum principle fails to give the optimal protocol and, in certain cases, the optimization problem may give rise to a so-called singular arc. In order to characterize the optimal solution completely, we thus need to investigate in greater detail the special case $h\,(1-\Phi) = \alpha/|\lambda|$.

A singular arc is defined by the requirement that the coefficient in front of the linear control term in the Hamiltonian $\mathcal{H}$ is zero for a finite time interval. In our problem this translates to the condition that $\alpha + \lambda\,h\,(1-\Phi) = 0$ on the singular arc. A necessary condition for this to happen is that all time derivatives of $\alpha + \lambda\,h\,(1-\Phi) = \partial\mathcal{H}/\partial r$ vanish on the singular arc, i.e.

$$\frac{d^k}{dt^k}\left(\frac{\partial\mathcal{H}}{\partial r}\right) = 0, \quad k = 0, 1, 2, \cdots \tag{S57}$$

Using Eq. (S19) with Eq. (S25) and Eq. (S26), we can rewrite condition Eq. (S57) for $k = 0, 1$ as:

$$k = 0: \qquad \frac{\partial\mathcal{H}}{\partial r} = \alpha + \lambda\,h\,(1-\Phi) = 0 \tag{S58}$$

$$k = 1: \qquad \frac{d}{dt}\left(\frac{\partial\mathcal{H}}{\partial r}\right) = \frac{d}{dt}\big(\alpha + \lambda\,h\,(1-\Phi)\big) = h\,\frac{d\lambda}{dt}(1-\Phi) - h\,\lambda\frac{d\Phi}{dt} = h\,(1 - \Phi - \alpha\gamma + f\lambda) = 0 \tag{S59}$$

We see that the condition for $k = 1$ is independent of the control r. As such, it can never be satisfied for all realizations of λ and Φ. Thus, no singular arc exists in our problem.

S3. Fluctuations of network failure times

We describe the distribution of failure times measured in our computer simulations (Fig. 1d,e of main text) using the Weibull distribution. The probability density function of the Weibull distribution is

$$p(x) = \frac{k}{\lambda}\left(\frac{x}{\lambda}\right)^{k-1} e^{-(x/\lambda)^k}. \quad [S60]$$

The average failure time is

$$\mu = \langle x \rangle = \frac{\lambda}{k}\Gamma\left(\frac{1}{k}\right). \quad [S61]$$

The variance in failure times is

$$\sigma = \langle x^2 \rangle - \langle x \rangle^2 = \frac{\lambda^2}{k^2}\left[2k\,\Gamma\left(\frac{2}{k}\right) - \Gamma\left(\frac{1}{k}\right)^2\right]. \quad [S62]$$

Hence the coefficient of variation is

$$C_v = \frac{\sigma}{\mu} = \frac{1}{\sqrt{2k\,\Gamma\left(\frac{2}{k}\right)/\Gamma\left(\frac{1}{k}\right)^2 - 1}}. \quad [S63]$$

In other words, the average and the standard deviation of the Weibull distribution are linearly correlated. The failure time distribution of aging networks is closely fitted by the Weibull distribution (Fig. 1e of main text) and a linear relationship between the mean and standard deviation of network failure times is also observed (Fig. 1f of main text).

S4. Computational model

S4.1. Network aging algorithm. The computational model constructs a network of N nodes according to the established programs for each corresponding network architecture (e.g. Gilbert random). The network has an initial vitality of $\phi_0 = 1 - d$ and is then subjected to an aging algorithm:

Algorithm 1 Aging

procedure AGE NETWORK(f, r, I)
  $\phi \leftarrow 1 - d$
  while $\phi > 0$ **do**
    for node x_i in the network **do**
      $x_i \leftarrow 0$ with probability f
      $x_i \leftarrow 1$ with probability r
    while $\exists$ node x_i with fraction of live neighbors $< I$ **do**
      for node x_i in the network **do**
        if fraction of live neighbors $< I$ **then** $x_i \leftarrow 0$
    $\phi \leftarrow \frac{1}{N}\sum_{i=1}^{N} x_i$

S4.2. Running the model. The network model of aging is implemented in Python 3. All of the code associated with the model, optimal repair protocol simulations and numerical solutions, and generation of figures is available at the corresponding Github repository for this paper. The repository provides example pipelines for generating all of the key figures in the main text and supplementary materials along with Python scripts containing the functions and methods for constructing, aging, and controlling complex networks. More information on the computational model is available in the repository.

S4.3. Summary of key model parameters. Here we outline some of the main parameters in the computational model. These parameters are arguments in the `simIndividual()` and `simPopulation()` methods in the `model.py` Python script, which simulate aging in a single complex network and a population of networks respectively. Information on other parameters can be found on the Github repository.

- `filename` [str]: root name for saving results and figures
- `pop_size` [int]: number of individuals to average results over in `simPopulation()`
- `N` [int]: number of nodes per individual network; default is 1000
- `p` [float]: probability of edges for random network; mean degree is $(N-1)p$
- `d` [float]: probability of initial failed state for each node; $\phi(t=0) \approx 1 - d$
- `f` [float]: independent probability of node failure; default set at $f = 0.025$
- `r` [float]: independent probability of node repair during repair period; default set at $r = 0.01$
- `f_thresh` [float]: threshold fraction of live nodes below which system failure occurs; default set at 0.1
- `graph_type` [str]: prefix of string input can be `scale_free` (for Barabasi-Albert scale free), `Grandom` (for Gilbert random), or `ERrandom` (for Erdos-Renyi random) with the suffix specifying directed (`_d`) versus symmetric/undirected (`_s`) graphs; default is `Grandom_s` (symmetric Gilbert random graph)

- `check_type` [str]: `none` (default) for uniform repair at rate `r` with no checking; `uniform` for checking each node at probability `P_check` before repair; `biased` for checking each node with probability as a function of degree
- `P_check` [float]: probability of checking a node; equivalent to c in the analytical model
- `repair_start` [int]: time T_1 at which repair or checking begins (used for bang-bang controls)
- `repair_end` [int]: time T_2 at which repair or checking ends (used for bang-bang controls)
- `time_end` [int]: time T at which simulation ends (convenient for calculating comparable costs during a time period);
- `dependency` [float]: critical fraction of vital provider nodes required to avoid automatic failure (e.g. if dependency is 0, then the network consists of independent nodes); this is equivalent to I in the analytical model

S4.4. Visualization of 2D aging network. A video file showcasing the aging process in a two-dimensional triangular lattice network ($N = 120$) is included in the supplementary materials. The final frame is shown in Fig. S4.

S5. Q-learning

Here we elaborate on the Q-learning algorithm that was used to approximate the optimal repair protocols from the analytic theory. The Q-learning model consists of a Q matrix containing values associated with each state-action pair where states correspond to the network vitality ϕ and actions correspond to repair options (e.g. $r(\phi) = r$ or $r(\phi) = 0$). A choice of action is made at each time step. With probability P_{exp}, the agent will explore an action by randomly choosing any of the actions available for that state with equal probability. With probability $1 - P_{\text{exp}}$, the agent will exploit the highest-valued action for the current state. The exploration probability decays with the number of training episodes as $P_{\text{exp}} = e^{-\lambda_{\text{exp}} q}$. The learning rate exponentially decays as $\beta = e^{-\lambda_\beta q}$. We used values of $\lambda_{\text{exp}} = 0.0005$ and $\lambda_\beta = 0.0005$, which were determined heuristically for runs of 15000 episodes. The corresponding state-action value in the table is updated according to the rule outlined in the main text:

$$Q(\phi_t, r_t) \leftarrow Q(\phi_t, r_t) + \beta[R_t + \gamma_Q \max_\rho\{Q(\phi_{t+1}, \rho)\} - Q(\phi_t, r_t)],$$

$$R_t = \phi_t - \alpha r_t.$$

We observed that 15000 episodes of Q-learning was sufficient for qualitative convergence to the optimal protocols as evidenced by the close matching to the analytic results. A detailed schematic representation of the Q-learning algorithm is shown in Fig. S5

S6. Alternative network structures

The results displayed in the main text correspond to the Gilbert random graph (3). The Gilbert random graph is also referred to as a $G(N, p)$ random graph since the probability of an edge between any two nodes of the network is p and there are N total nodes in the network. We construct the Gilbert network by initializing an unconnected set of N nodes and then drawing edges between each pair of nodes with probability p.

The results for the linearized model (i.e. where there are no interdependencies between the components of a network and $I = 0$) hold true regardless of network structure. However, in the nonlinear model where $I > 0$, different network structures may present different aging dynamics. Here we explore two common network structures, the Erdos-Renyi random graph (4) and the Barabasi-Albert scale-free graph (5), and show that they produce highly similar cascading failure behavior and observe comparable optimal repair protocols relative to the Gilbert model results outlined in the main text.

S6.1. Erdos-Renyi. The Erdos-Renyi (ER) random graph is constructed by building a network from the first node onward. Each subsequent node forms an edge with a pre-existing node with probability that decreases with node degree (k_j). ER graphs are also referred to as $G(N, m)$ random graphs where a network is randomly chosen from the set of all networks with N nodes and m edges. We construct the ER random network using the NetworkX implementation (6).

ER random networks exhibit a characteristic failure cascade (see Fig. S6a) that was also observed in Gilbert random networks. The dependence of the critical failure time t_c on the interdependence I is very similar to that of the Gilbert random model (see Fig. S6c). Further, the optimal repair protocols match the numerical solutions for different values of I and are similar to the optimal protocols in the Gilbert network (see Fig. S6d).

S6.2. Barabasi-Albert. The Barabasi-Albert (BA) scale-free graph can be constructed in two ways (with highly similar end results). The first method is through the NetworkX implementation of a BA graph, which is the default option in `model.py`. The second method is to manually build the network one node at a time. For the first pN nodes, a fully-connected network is formed meaning that each node is connected to every other node. After that, each subsequent node added forms an edge with an existing node with probability proportional to node degree k:

$$P(E_{ij}) = \frac{k_j}{\sum_n k_n}$$

The BA model results in a scale-free distribution of degrees where $P(k) \sim \frac{1}{k^3}$ is the probability of a given module having k interdependencies. We construct the BA scale-free network using the NetworkX package (6).

BA scale-free networks produce highly similar cascading failure behavior and critical failure time t_c distributions as compared to either of the two random networks (see Fig. S6bc). The optimal repair protocols for scale-free networks are also similar to those of random networks (see Fig. S6e).

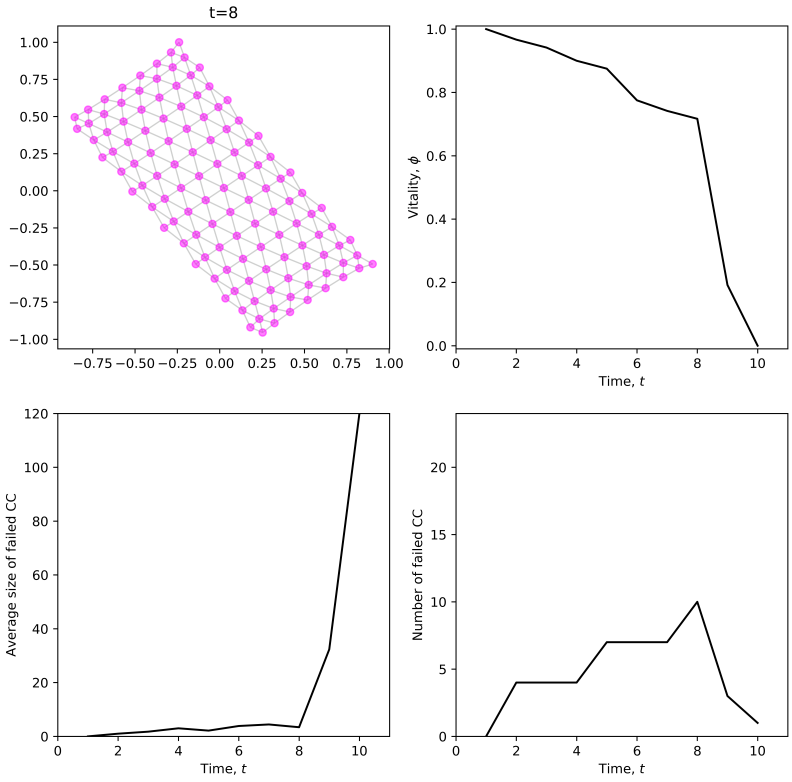

Fig. S4. 2D network failure visualization. Final state of node failure and cascade in a two-dimensional triangular lattice network of size $N = 120$. Full video visualization is in additional materials. The upper left panel displays a live visualization of the network where nodes are colored cyan (functional) and magenta (failed). The upper right panel displays the corresponding vitality ϕ as a function of time. The bottom left panel displays the average size of the connected subgraphs of failed components, and the bottom right panel displays the number of these connected subgraphs of failed components. The aging parameters are $f = 0.025$, $r = 0$, $I = 0.6$.

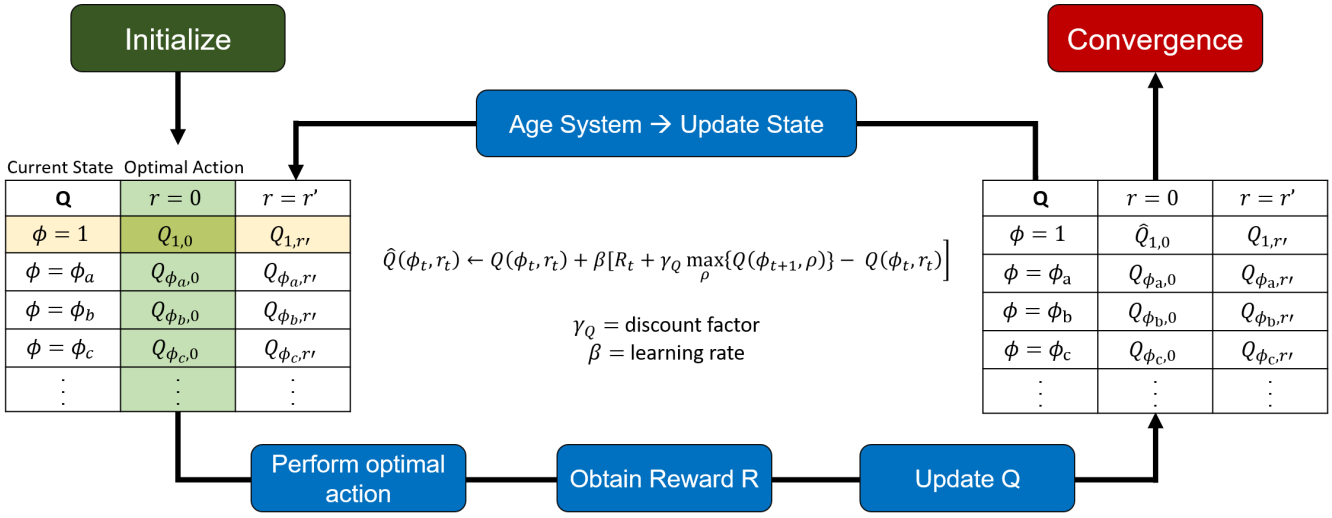

Fig. S5. Schematic representation of the Q-learning algorithm used in developing adaptive optimal controls for aging in the network model.

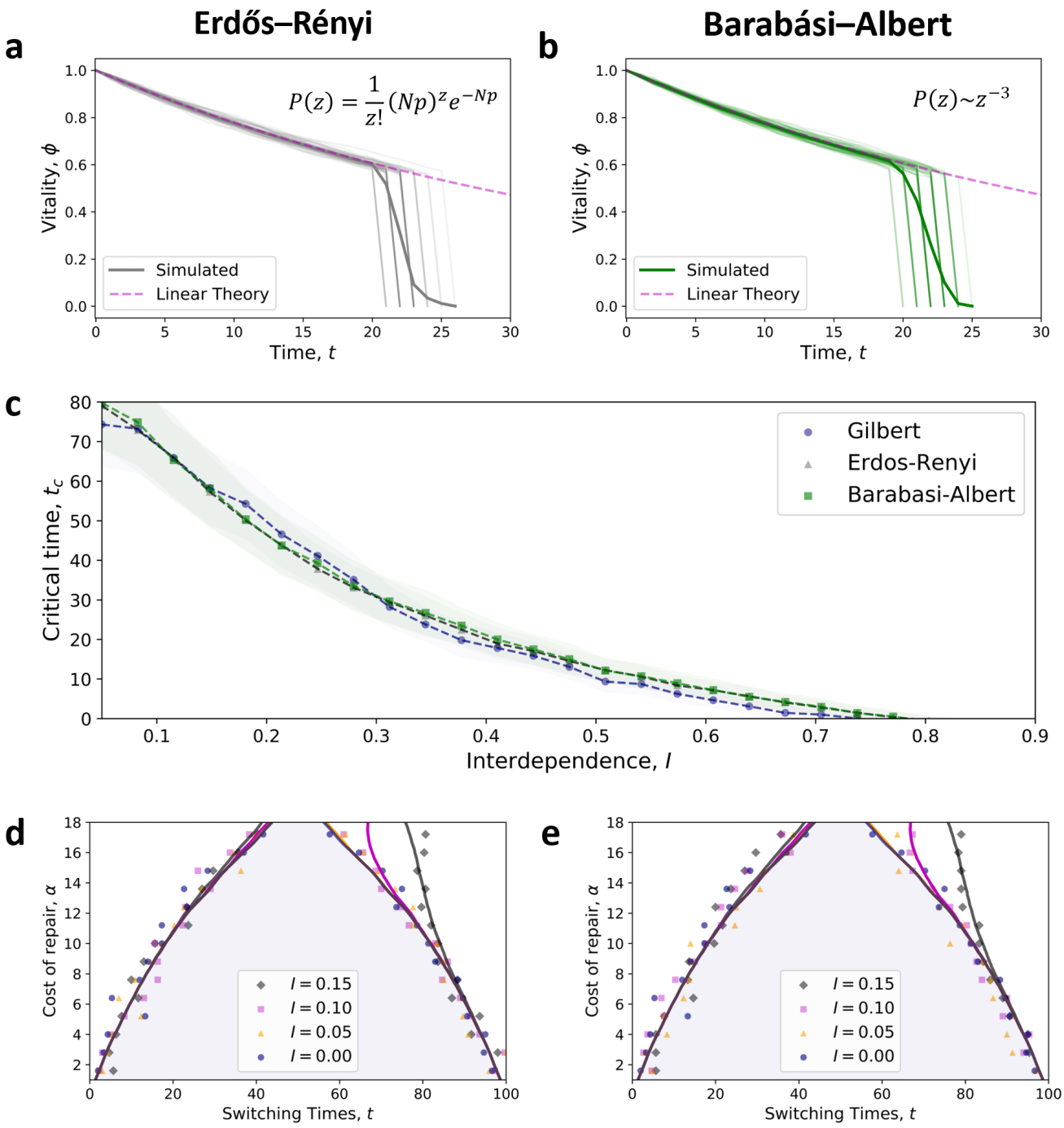

Fig. S6. Aging and optimal control in Erdos-Renyi and Barabasi-Albert networks. (a) Vitalities $\phi(t)$ of Erdos-Renyi random graphs and (b) of Barabasi-Albert scale-free graphs follow similar cascading failure trajectories with time as observed in the Gilbert model. Parameter values in (a) and (b) are identical to those used in Fig. 1b. (c) Distribution of critical failure times t_c as a function of interdependence I for Gilbert, Erdos-Renyi, and Barabasi-Albert networks are nearly identical. The shaded regions correspond to one standard deviation from the mean t_c obtained from averaging over 200 networks. Parameters used were the same as in (a) and (b). (d) Nonlinear ($I \geq 0$) optimal repair protocols for the $\gamma = 0$ cost function in Erdos-Renyi networks and (e) Barabasi-Albert networks as compared to the numerical solutions. We solved for the numeric optimal policies in Figure using the `ezsolve` function in the TOMLAB/POPT Matlab package, which was also used for the numeric solutions in Figure 2E of the main text.

S7. Model fitting to *C. elegans* data

Values for f, r, I, and α are required to fit the network model to empirical data and determine a unique optimal repair protocol. Here we fit our network model to two different cohorts of *C. elegans* (treated versus vehicle) (7) to obtain estimates of f, r, and I. The cost of repair α was left as a free parameter because real-world interpretation of the cost is subjective and requires data that is not readily available (e.g. toxicity of α-ketoglutarate treatment). We bootstrap-fitted (100 bootstraps) the failure time distributions of 10^5 networks ($N = 200$, $p = 0.1$) to *C. elegans* lifespans by minimizing the Kolmogorov–Smirnov distance between the two distributions. Estimates of $f = 0.004$ and $I = 0.8$ were obtained from fitting the model to 306 vehicle *C. elegans* lifespans using a numerical grid search (Fig. S7a). These values were then used to fit the model to 297 treated *C. elegans* lifespans to estimate $r = 0.043$ from a numerical line search (Fig. S7b).

S8. Alternative cost functions

S8.1. Cost function with Φ-dependent repair rate. In systems that undergo self-repair (e.g. cellular turnover, wound healing, auto-maintenance), the efficacy of the repair mechanism is often linked to the quality of the system such that a decrease in the vitality is likely to result in less efficacious self-repair. To model the cost function in these self-repairing systems, we make the repair rate dependent on the vitality Φ. We can repeat our optimal control calculation using the alternative cost function

$$\text{Cost} = \int_0^T e^{-\gamma t}\big[\alpha r(t)(1-\Phi(t)) - \Phi(t)\big]\,dt, \tag{S64}$$

where γ is the discount rate and α is the relative cost of repair. This cost function reflects the fact that the repair rate depends on the current fraction of failed nodes.

S8.1.1. Solution to optimal control problem. To solve the optimal control problem, we introduce the current Hamiltonian

$$\mathcal{H} = \alpha r(1-\Phi) - \Phi + \lambda\big[r_{\text{tot}}(1-\Phi) - f_{\text{tot}}\Phi\big], \tag{S65}$$

where $\lambda(t)$ is a co-state variable. The optimal protocol is determined by minimizing $\mathcal{H}$ with respect to the control r, yielding

$$\frac{\partial \mathcal{H}}{\partial r} = 0 \quad \Rightarrow \quad \alpha + \lambda\, h = 0. \tag{S66}$$

The optimal control is thus a bang-bang control that switches between $r(t) = 0$ and $r(t) = r$

$$r(t) = \begin{cases} r, & h > \alpha/|\lambda| \\ 0, & h < \alpha/|\lambda| \end{cases} \tag{S67}$$

The equation for the co-state variable λ is

$$\frac{d\lambda}{dt} = \gamma\lambda - \frac{\partial \mathcal{H}}{\partial \Phi} = 1 + \alpha r + (\gamma + f_{\text{tot}} + r_{\text{tot}})\lambda + \lambda\,\Phi\,\frac{\partial f_{\text{tot}}}{\partial \Phi} - \lambda(1-\Phi)\,\frac{\partial r_{\text{tot}}}{\partial \Phi}, \tag{S68}$$

with $\lambda(T) = 0$.

S8.1.2. Linearized control problem. We can obtain an explicit expression for the switching time by considering the linearized limit. In this case, the equation for for λ, Eq. (S68), becomes

$$\frac{d\lambda}{dt} = 1 + \alpha r + (\gamma + f + r)\lambda. \tag{S69}$$

For $t > T_2$, we have $r(t) = 0$, and the solution for λ is

$$\lambda(t) = \frac{e^{(f+\gamma)(t-T)} - 1}{f + \gamma}, \quad T_2 < t. \tag{S70}$$

The switching time T_2 is then determined as to the following equation

$$\lambda(T_2) = \alpha \quad \Rightarrow \quad \frac{e^{(f+\gamma)(T_2-T)} - 1}{f + \gamma} = \alpha. \tag{S71}$$

The solution for the switching time is:

$$T_2 \simeq T - \frac{1}{f+\gamma}\log\left[1 + \alpha(f+\gamma)\right]. \tag{S72}$$

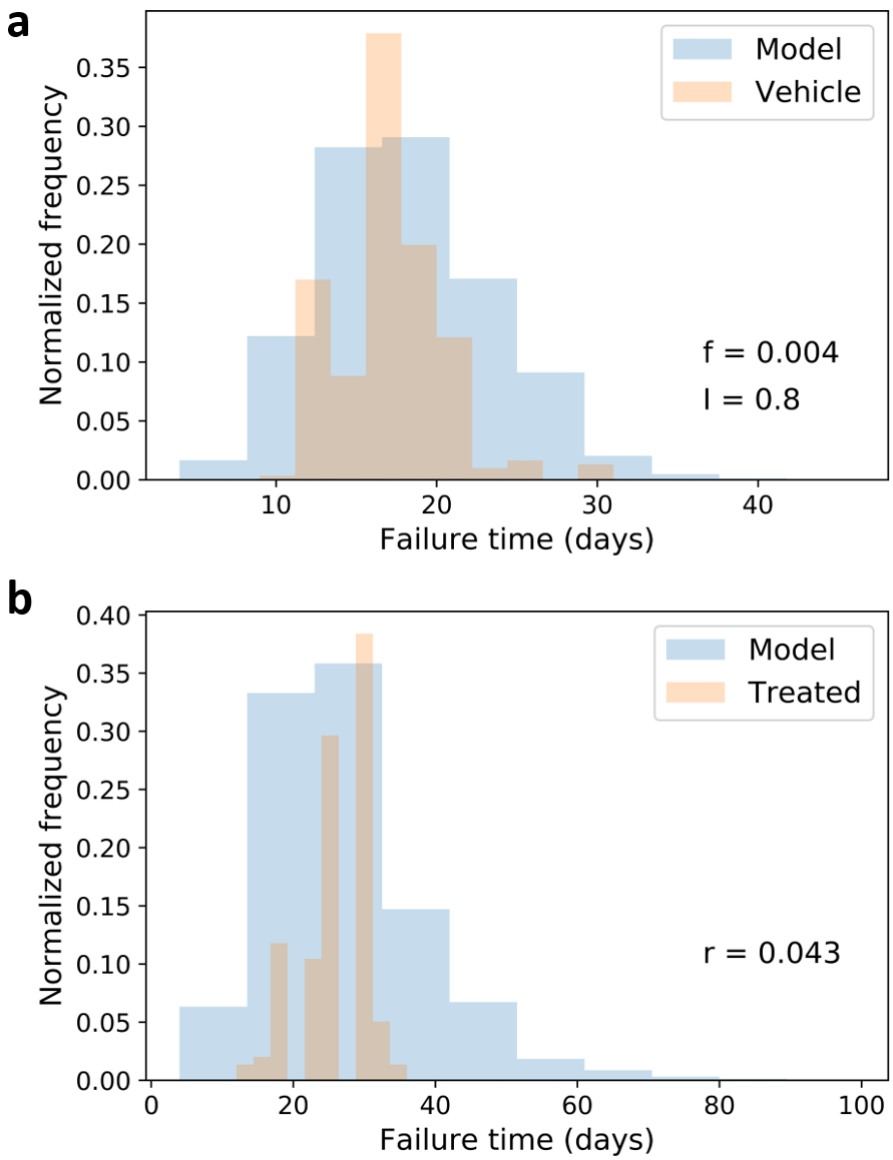

Fig. S7. Failure time distributions of fitted models and *C. elegans* treatment groups. (a) Model with closest failure time distribution to that of the vehicle control group. Bootstrap-fitted parameters were $f = 0.004$ and $I = 0.8$. (b) Model with closest failure time distribution to that of the α-ketoglutarate treatment group given fitted f and I. Bootstrap-fitted repair rate was $r = 0.043$.

S8.2. Quadratic cost of repair. The optimal control problem discussed in the main article yields a bang-bang control as solution. This is due to the fact that the cost function Eq. (S17) is linear in the repair frequency. The resulting optimal control selects the maximal possible value of r out of an interval of possible repair frequencies $[0, r]$. In this section, we illustrate how optimal protocols can be determined for nonlinear cost functions. We illustrate this idea for the example of a cost function that is quadratic in the repair rate $r(t)$:

$$\text{Cost} = \int_0^T \big[\alpha r(t)^2 - \Phi(t)\big] dt. \tag{S73}$$

We solve the resulting optimal control problem by considering the following Hamiltonian function

$$\mathcal{H} = \alpha r^2 - \Phi + \lambda\big[r - (f + r)\Phi\big], \tag{S74}$$

where $\lambda(t)$ is a co-state variable. The optimal protocol is determined by minimizing $\mathcal{H}$ with respect to the control r

$$\frac{\partial \mathcal{H}}{\partial r} = 0 \quad \Rightarrow \quad r = \frac{\lambda(\Phi - 1)}{2\alpha}. \tag{S75}$$

Note that, in this case, the optimal control is no longer bang-bang, but is set by the time evolution of the functions $\Phi(t)$ and $\lambda(t)$. From this equation it is clear that the repair rate must be zero at the start and at the end of the protocol. This follows from the fact that $\Phi = 1$ at the start and $\lambda = 0$ at the end. The functions Φ and λ obey the following differential equations

$$\frac{d\Phi}{dt} = \frac{\partial \mathcal{H}}{\partial \lambda} = r - (f + r)\Phi = -\frac{\lambda(1 - \Phi)^2}{2\alpha} - f\Phi, \tag{S76}$$

with initial condition $\Phi(0) = 1 - d$, respectively,

$$\frac{d\lambda}{dt} = -\frac{\partial \mathcal{H}}{\partial \Phi} = 1 + (f + r)\lambda = 1 + f\lambda + \frac{\lambda^2(\Phi - 1)}{2\alpha}, \tag{S77}$$

with the boundary condition $\lambda(T) = 0$ (transversality condition). We solved Eq. (S76) and Eq. (S77) numerically and used Eq. (S75) to determine the optimal repair protocol; the result is shown in Fig. S8. Even though the optimal protocol is no longer bang-bang, it still features regions of low repair near $t = 0$ and $t = T$ and a region of large repair in the middle.

S9. Optimal control problem with checking

Here we discuss a potential extension of the optimal control problem discussed in the main text by adding a checking step before repair is performed. In this case, each node is checked with rate c; checked nodes are then repaired with probability β. There is a time delay between checking and repair. The net repair rate r is then described in the simplest scenario as:

$$\frac{dr}{dt} = -\frac{(r - \beta c)}{\tau}, \tag{S78}$$

where τ is the delay between repair and checking. This equation has the fixed point $r = \beta c$. Thus, for a non-vanishing checking rate $c \neq 0$ repair will increase over time and reach the plateau βc. When $c = 0$, the fixed point becomes 0. Note that when the delay τ is very small, the exponential decay/increase of r in response to c will be very sharp; the repair rate then approaches a step function where $r = 0$ for $c = 0$ and $r = \beta c$ for $c \neq 0$.

S9.1. Definition of optimal control problem with checking. The optimal control problem with a checking step included reads

$$\frac{d\Phi}{dt} = -f\Phi + r(1 - \Phi), \tag{S79}$$

$$\frac{dr}{dt} = -\frac{(r - \beta c)}{\tau}. \tag{S80}$$

The control variable in the problem is now $c(t)$ (the control protocol) and no longer r (since r is "slaved" to c through the new differential equation). The goal of the optimal control problem is to determine this checking control $c(t)$ such that the cost for checking and repair is minimized and the integrated vitality is maximized:

$$\text{Cost} = \int_0^T \big[\alpha_1 c(t) + \alpha_2 r(t) - \Phi(t)\big] dt, \tag{S81}$$

where α_1 and α_2 are the relative costs for checking and repair.

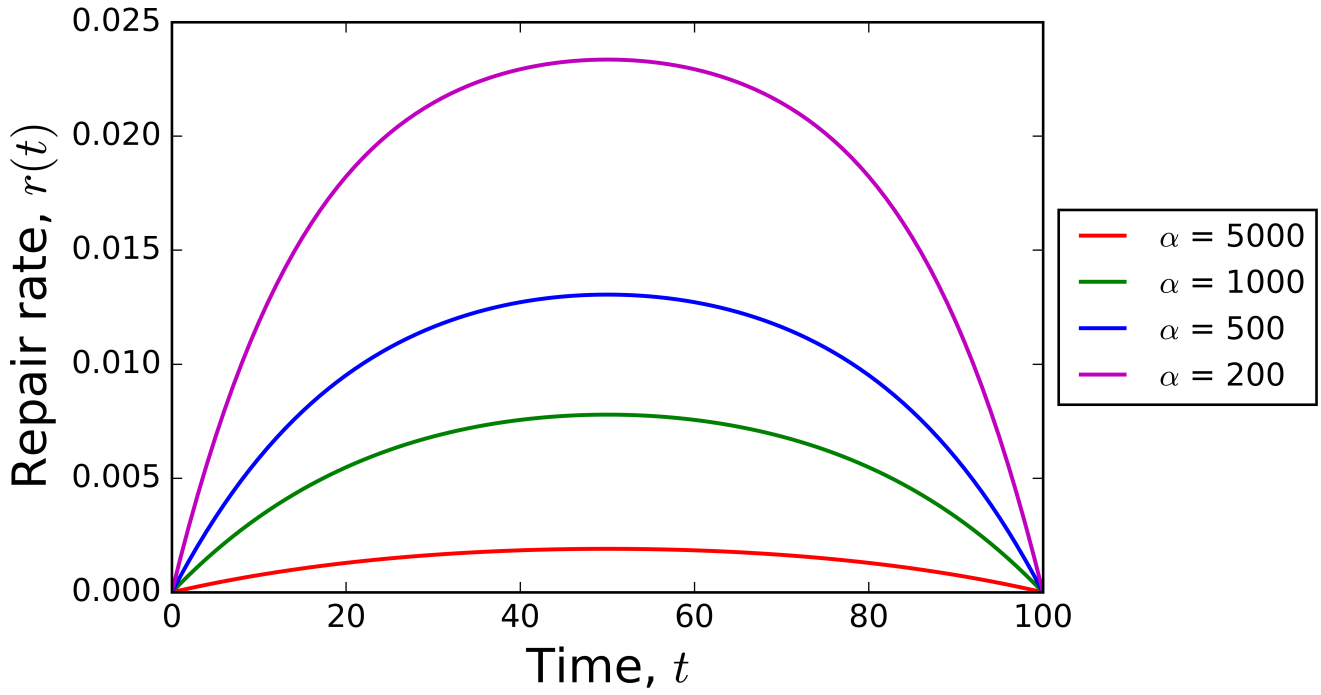

Fig. S8. Optimal repair $r(t)$ protocols for the quadratic cost functional. Protocols are shown for different costs of repair α. The protocols are characterized by a middle region of highest repair and flanked by regions of lower repair at early and late times. Parameters are $N = 1000$, $f = 0.025$, $I = 0$, $d = 0$, $p = 0.1$, and $T = 100$.

S9.2. Solution to optimal control problem with checking. To solve the optimal control problem given by Eq. (S79) and Eq. (S81) we consider the following Hamiltonian function

$$\mathcal{H} = \alpha_1 c + \alpha_2 r - \Phi + \lambda_1 \left[\frac{\beta c}{\tau} - \frac{r}{\tau}\right] + \lambda_2 \big[r - (f+r)\Phi\big], \tag{S82}$$

where $\lambda_1(t)$ and $\lambda_2(t)$ are co-state variables. The optimal protocol is determined by minimizing $\mathcal{H}$ with respect to the control c

$$\frac{\partial \mathcal{H}}{\partial c} = 0 \quad \Rightarrow \quad \alpha_1 + \lambda_1 \frac{\beta}{\tau} = 0. \tag{S83}$$

The optimal control is thus a bang bang control that switches between $c(t) = 0$ and $c(t) = c$ depending on the sign of $\alpha_1 + \lambda_1 \frac{\beta}{\tau}$. If $\alpha_1 + \lambda_1 \frac{\beta}{\tau} > 0$, we have $c(t) = 0$, while if $\alpha_1 + \lambda_1 \frac{\beta}{\tau} < 0$, we have $c(t) = c$. Thus

$$c(t) = \begin{cases} c, & \lambda_1 < -\frac{\alpha_1 \tau}{\beta} \\ 0, & \lambda_1 > -\frac{\alpha_1 \tau}{\beta} \end{cases} \tag{S84}$$

The optimal control protocol will thus be of the form

$$c(t) = \begin{cases} 0, & t < T_1 \\ c, & T_1 < t < T_2 \\ 0, & T_2 < t \end{cases} \tag{S85}$$

To find the switching times, we solve for the functions λ_1, λ_2, r and Φ. The equations for Φ and r are

$$\frac{dr}{dt} = \frac{\partial \mathcal{H}}{\partial \lambda_1} = -\frac{(r - \beta c)}{\tau} \tag{S86}$$

$$\frac{d\Phi}{dt} = \frac{\partial \mathcal{H}}{\partial \lambda_2} = r - (f+r)\Phi \tag{S87}$$

with initial conditions $r(0) = 0$ and $\Phi(0) = 1$. The equations for λ_1 and λ_2 are

$$\frac{d\lambda_1}{dt} = -\frac{\partial \mathcal{H}}{\partial r} = \frac{\lambda_1}{\tau} + \lambda_2(\Phi - 1) - \alpha_2 \tag{S88}$$

$$\frac{d\lambda_2}{dt} = -\frac{\partial \mathcal{H}}{\partial \Phi} = 1 + (f+r)\lambda_2 \tag{S89}$$

with the boundary conditions $\lambda_1(T) = \lambda_2(T) = 0$ (transversality condition). The solution for the repair protocol is

$$r(t) = \begin{cases} 0, & t < T_1 \\ \beta c\big(1 - e^{-(t-T_1)/\tau}\big), & T_1 < t < T_2 \\ r(T_2) e^{-(t-T_2)/\tau}, & t > T_2 \end{cases} \tag{S90}$$

Note that for $\tau \to 0$, we recover

$$r(t) = \begin{cases} 0, & t < T_1 \\ \beta c = r, & T_1 < t < T_2 \\ 0, & t > T_2 \end{cases} \tag{S91}$$

which is Eq. (S24). Using Eq. (S90) and applying a perturbation expansion in τ, we obtain the following expressions for the switching times:

$$T_1 \simeq \frac{1}{f} \log\left[\frac{1 - \tau(f+r)}{1 - \tau r - \alpha(f+r)}\right] \tag{S92}$$

and

$$T_2 \simeq T - \frac{1}{f} \log\left[\frac{1 + (r+f)\tau}{1 + \tau r - \alpha(r+f)}\right], \tag{S93}$$

where $r = \beta c$ and $\alpha = \alpha_2 + \frac{\alpha_1}{\beta}$. For $\tau = 0$, Eq. (S92) and Eq. (S93) recover Eq. (S33) and Eq. (S34).

References

1. Vural DC, Morrison G, Mahadevan L (2014) Aging in complex interdependency networks. *Physical Review E* 89(2):022811.
2. Hocking LM (1991) *Optimal Control: An Introduction to the Theory with Applications*. (Clarendon Press). Google-Books-ID: gd7b4FMqXpMC.
3. Gilbert EN (1959) Random Graphs. *The Annals of Mathematical Statistics* 30(4):1141–1144.
4. Erdős P, Rényi A (1960) On the Evolution of Random Graphs. *Publ. Math. Inst. Hung. Acad. Sci* p. 45.
5. Barabási AL, Albert R (1999) Emergence of Scaling in Random Networks. *Science* 286(5439):509–512.
6. Hagberg A, Swart P, Chult DS (2008) Exploring network structure, dynamics, and function using networkx. *The U.S. Department of Energy's Office of Scientific and Technical Information* LA-UR-08-05495.
7. Chin RM, Fu X, Pai MY, Vergnes L, Hwang H, Deng G, Diep S, Lomenick B, Meli VS, Monsalve GC, Hu E, Whelan SA, Wang JX, Jung G, Solis GM, Fazlollahi F, Kaweeteerawat C, Quach A, Nili M, Krall AS, Godwin HA, Chang HR, Faull KF, Guo F, Jiang M, Trauger SA, Saghatelian A, Braas D, Christofk HR, Clarke CF, Teitell MA, Petrascheck M, Reue K, Jung ME, Frand AR, Huang J (2014) The metabolite α-ketoglutarate extends lifespan by inhibiting ATP synthase and TOR. *Nature* 510(7505):397–401